Czech University of Life Sciences Prague

Faculty of Engineering

Behaviour of Agricultural Products in High Hydrostatic Pressure Regimes

Doctoral Thesis

Department of Mechanical Engineering

Supervisors: prof. Ing. Radomír Adamovský, DrSc.

prof. Ing. RNDr. Jiří Blahovec, DrSc.

RNDr. František Mošna, Ph.D

Doctoral Student: Olaosebikan Layi Akangbe, M.Sc

Prague 2019

Declaration

I declare that the work in the thesis entitled ‘Behaviour of Agricultural Products in High Hydrostatic Pressure Regimes’ has been performed by me under the supervision of prof. Ing. Radomír Adamovský, DrSc., prof. Ing. RNDr. Jiří Blahovec, DrSc. and RNDr. František Mošna, Ph.D. The information derived from literature has been duly acknowledged in the text and a list of references provided. No part of this thesis was previously presented for another degree or diploma at any University.

………………………………………………….

In Prague February 6, 2019 (Olaosebikan Layi Akangbe)

Acknowledgment

My sincere gratitude to the members of my supervisory team, prof. Ing. Radomír Adamovský, DrSc., prof. Ing. RNDr. Jiří Blahovec, DrSc. and RNDr. František Mošna, Ph.D. who patiently meticulously guided me through this work; also to the Head of the department of Mechanical Engineering and all members of Faculty who were of assistance in the course of the work in one way or another. The studies reported here were funded through the Internal Grants Agency of the Faculty of Engineering of the Czech University of Life Sciences, Prague.

Abstract

In this study, exponential functions for estimating densification requirements for whole seeds and powdered forms of *Lens culinaris* Medik. and *Cicer arietinum* L. in regions of high hydrostatic pressures ranging between 50-500 MPa and at a deformation rate of 5.5 $mm.min^{-1}$, given depths of product charge corresponding to an aspect ratio of 0.5 at product moisture contents of approximately 12% , in dry basis, were established. A 4 X10 full factorial experiment fitted into a completely randomised design for the analysis of variance and comparison of treatment means using Duncan's multiple range test was adopted. Both product form and applied pressure had highly significant effects on mechanical response in the compressed materials, except for the effects of pressure on the rate of strain, and of the interaction of the forms of the product with applied pressure on strain rate and the time to peak deformation. The modified Gompertz function was found to provide a proper fit for pressure-density relationship (R^2=0.99). All the parameters of this model had highly significant effects in estimating the pressure as a function of density. The effect of the model at predicting this behaviour was found to be highly significant ($p<0.0001$). The development of radial or lateral wall pressure during compression presented a very steep slope, at the initial stages and a much gentler slope in the pressure range between 400-500 MPa. Gain in bulk density appreciated with increased magnitude of applied pressure and was higher for whole seed forms than for powders. Energy requirement for compressing these materials increased as did the magnitude of applied pressure and varied for the different product forms, being lower for powders than for whole seeds; the time rate of expenditure of energy for every unit mass of material was however greater for powders than for whole seeds. Mean compressed product densities of between 1277.6-2060.6 $kg.m^{-3}$ were achieved with the range of pressure employed. When the combined effects of pressure, the time rate of deformation and aspect ratio were considered, at applied pressures of 50 and 100 MPa, deformation rates of 5.5, 10 and 14.5 $mm.min^{-1}$ and aspect ratios of 0.5, 1.0 and 1.5 with *Ceratonia siliqua* L., at 4.81% moisture content, in dry basis, mechanical response was found to be affected significantly by the different levels of each of these factors and by their interactions. The rate of strain and specific power requirement for the densification of this product were found to be power functions of the aspect ratio, at all rates of deformation. Gain in bulk density was found to be better at the lower aspect ratios. However, energy efficiency improves significantly as aspect ratio increases. The findings in this study are of direct relevance to the development of modified food forms. Immediate applications are with respect to combined high pressure and short duration high temperature edible snack and cereals production systems. Mechanical behavior of biomaterials given high pressures is of importance in postharvest product handling, storage and food processing.

Keywords: hydrostatic pressure, strain, deformation, compressibility, bulk density

Table of Contents

List of Tables

List of Figures

List of Plates

List of Appendices

Abbreviations, Symbols, Definitions and Glossary

*	significant effect
**	highly significant effect
$\dot{\bar{\omega}}_{\rho}$	specific power, W.kg^{-1}
$\bar{p}_T$	radial or lateral pressure acting on wall of the vessel
$\bar{p}'_x$	axial pressure in the compressed material
$\bar{\omega}_{\bar{\rho}}$	mass specific energy requirement, J.kg^{-1}
$\dot{E}$	Volume specific energy demand, J.mm^{-3}
E_v	Volume specific deformation energy, J.m^{-3}
F_0 , F_1	force acting on the material at two positions, 0 and 1
F_n	compressive forcefor a known deformation, N
F_s	radial force, N
F_t	force of friction, frictional drag, N
G_ρ	gain in bulk density, %
H_o	initial depth of product in the compression chamber, mm
V_{ff}	free–fill volume, mm^3
i_1 , i_2	porosities associated with ρ_p and ρ_s, respectively
p_a	effective applied pressure, Pa
p_s	radial, lateral or side pressure, Pa
r_a	aspect ratio, -
r_d	time rate of deformation, mm.s^{-1}
r_f	friction ratio, -
t_c	time to compression, *s*
t_c	time to deformation, s
δ_c	achieved deformation, mm
δ_n	known deformation, mm
ρ_1, ρ_2	initial product density and attained density, kg.m^{-3}
ρ_b	bulk density, kg.m^{-3}
ρ_c	bulk density of compressed material, kg.m^{-3}

ρ_o initial bulk density, kg.m^{-3}

ρ_s density of cell wall material, kg.m^{-3}

ρ_t true density kg.m^{-3}

$\dot{\epsilon}$ rate of strain, s^{-1}

μ friction coefficient

b, c, m, n proportionality and exponential constants

D the diameter of the elemental disc,

K_O initial bulk modulus

m_c mass of compressed material, g

ns none statistically significant effect

P_f porosity, (%)

P_x compression pressure at x

V_c Final volume of material after compression, mm^3

D internal diameter and characteristic dimension of the compression vessel, mm

F applied compression force, N

F, F_S and F_t applied normal, lateral and friction forces, respectively

R proportion of solid in the matrix

V initial volume of compressed material, mm^3

a cross-sectional area of the compressed disc

dF elemental force, N

dx the thickness of the elemental disc of material

e base of the natural logarithm

i number of subdivisions of the deformation axis

i porositiy

l Depth of compressed product, mm

m mass of compressed material, kg

p applied axial pressure, Pa

u surface area of the elemental disc of the material in contact with the wall of the die

w specific work, J.kg^{-1}

γ, γ_o Bulk density, initial bulk density, kg.m^{-3}

δ deformation, mm

μ wall friction coefficient, -

μ, μ_w and μ_k friction coefficient, coefficient of wall friction and coefficient of kinetic friction $\mu\xi$

side pressure factor

ξ pressure ratio, -

ρ density, kg.m^{-3}

τ shear resistance at the material-wall interface, Pa

ϵ Strain in the compressed material, -

1. Introduction

1.1. Brief Overview

Product densification is an important unit operation in agriculture and its relevance and application spans not only production activities but also product handling, transport, storage and manufacturing. This phenomenon determines, to a very good extent, the effectiveness with which feed and food materials may be prepared in the field, how much modification occurs in them during handling and transport, the forms and capacity by which they may be transported, the efficiency of postharvest preservation and storage systems through which they may be passed, modifications that may be had and constraints which may be encountered when adapting the processes involved for the derivation of desirable product forms. This technique may be successfully applied to the development of new food, feed and nutraceutical products, especially in mass production schemes. The outcomes would include ready to eat and functional foods and products such highly densified or expanded food cakes and natural nutrient supplements. The procedure may be applied to achieving and retaining quality during the production of food products as well as the elimination of undesirable contents and properties, when combined with some other known techniques.

Densification, expression and extrusion are three activities which involve product compression. In order to achieve one or any combination of these, states of stress are normally induced to cause reductions in the sizes of elemental materials or particles of the products, modify their textural or constitutional properties and generate both compact and/or consolidated product forms in preferred presentations. Other aspects where this understanding is relevant include the production of briquetted and agglomerated product forms. Broad advantages abound in understanding the natures of these products and feedstocks as well as their responses to physical, process and load treatments. In most systems, a combination of loads is necessary to effectuate densification, including axial compressive, shear and torsional loads. The major influence of interest is compressive stress. Indirect contributions of such effects as frictional resistance are perceivable but not exhaustively in heat load transforms, necessitating their study. The effects of this are variedly faceted, including thermally induced modifications of physico-chemical properties of the end product which influence mechanical response and effects on the processing system.

1.2. Problem Statement

The behaviour of agricultural products in all-round pressure regimes has not been totally described. Although different empirical forms may be found [1–4], most of these exist with respect to fibrous materials [5] and were concerned, mainly with relating applied pressure to initial and relaxed product densities. Very scanty treatments of the subject may be found for solid or granular agricultural materials. Treated forms for fibrous materials include exponential and power relations as well as treatments based primarily on theoretical concepts of the loss of void capacities. These different forms have been shown to dominate different regions of influence [5, 6] characterised essentially by the magnitudes of applied pressure. Power functions were shown to be quite useful in explaining response in high pressure zones [7]. The boundaries of these activities are however not precise but constitute some ranges. Effects of reported models tend to vary, even within their established domains of relevance, and they are sensitive to property and process conditions [7]. For example, fluctuations of pressure with varying moisture are exponential in form. As a result, authors adopt multiphased description and segmented interpretations of the behaviours of agricultural materials under load.

Functional forms can be arrived at which express the behaviours of agricultural products in terms of the relevant physical, mechanical and process parameters involved during states of stress which are normally induced to achieve desirable densified and derived product forms, particularly given hydrostatically applied loads. The object of this study is to develop an understanding of these responses for a few select agricultural food, feed and medicinal crops, namely *Ceratonia siliqua* L., *Lens culinaris* Medik. and *Cicer arietinum* L.

1.3. Justification of the Study

Product densification is applied in unit operations and processes involving the production of many food, nutritional supplements, feed and solid fuel. The study will provide deep insight into the mechanism of densification of agricultural products and of their responses given variations in physical, machine and process parameters. Functional forms generated in the course of this study will provide rational basis for equipment design and development as well as optimised operation of such equipment.

1.4. Objectives of the Study

The general objective of this study shall be to determine the behavior of selected agricultural products in high hydrostatic pressure regimes.

The specific objectives shall include:

1. To determine functional forms fitting the behaviour of the selected agricultural products in high hydrostatic pressure regimes
2. To verify these functional forms and validate them using acceptable standard procedure
3. To optimise for mechanical response based on select criterion variable(s)

1.5. Scope and Limitations of the Study

In this study, the behaviour of selected agricultural products and performance during high pressure hydrostatic compression shall be investigated. The study shall exclude all thermal and chemical influences. Compressive stresses shall be steadily induced and no dynamic events shall be involved.

2. Literature Review

2.1. High Pressure Hydrostatic Compression (HPHC): Principle and Economic Importance

Bulk compression of agricultural products is carried out with a view to enhancing the bulk, nutrient and calorific densities of such materials to improve food and feed performance, transportability and storage [8]. Densification based systems are implemented in industry in different processes for creating numerous food [9, 10], nutraceuticals [11] and feed forms and for enhancing their qualities and abilities to store. Compressive stress may therefore be oriented at occasioning productive material element failure [12], achieving compact forms and sterilisation. Techniques adopted for these industrial operations are implemented using very high hydrostatic pressures. High pressure hydrostatic compression may be exploited to achieve desirable material behaviours applicable to foods and the development of advanced engineering materials; such materials capable of negative strains in high hydrostatic stress regimes [13] are of particular importance in this regard. Other applications of this include low temperature, high pressure product quality retention, enhancement and sterilisation schemes [14, 15].

Densification of plant materials is a complex process [16] and the properties which characterise it vary under different conditions [17, 18]. Agricultural materials are heterogeneous in nature. This means that stress related behaviours vary with products and their conditions, as well as with processing conditions. Additional complexities attend response in pre-treated and formulated products which are often handled to create new food, supplements and feed forms; mixed or composite biomaterials possess properties and exhibit behaviours which are at variance with those of the individual constituent materials [19, 20]. Understanding these qualities is vital to achieving precise and optimum design of machine elements and components involved in the related unit operations.

2.2. HPHC Systems, Mechanisms and Applications

Various forms of product densification systems are reported [21]. They include the batch and continuous process systems such as hydraulic/piston, briquette, screw, pelletize and roller systems. The predominant action in each unit is compression of fed biomaterial. As such, it is possible to carefully relate densification activities in each of these systems.

2.3. Mechanism of Hydrostatic Compression of Biomaterials

Densification of porous agricultural material is a process of compression which is attended with the effects of friction along the walls of the pressure vessel and inhomogeneous distribution of pressure and bulk density [6]. Authors appear to be agreed on the mechanism of phenomenon [1, 7, 22]. Bulk columns of plant materials constrained in pressure vessels under hydrostatic conditions are compressed, axially and a state of stress is induced, triaxially. Radial constraints are applied through retaining walls while productive stress is normally applied, along the longitudinal axis of the constraining vessel, perpendicular to its radius. A distribution of stress along the diametral span of the sectioned compressing plate has been suggested [1, 23, 24]. The distribution of the applied pressure along the compression axis is little understood. There are indications this would vary with product depth and the variation would constitute a stress transmission factor [1]. Bulk agricultural materials may be seeds, fruits, fibres or particulates. These elemental units and the voids between them constitute bulk material matrices. Under compression, a rearrangement in the matrix first occurs as elemental units slide and roll to occupy available voids [2, 25]. When sufficient contacts are established, and stress transmission induced between the elements, the material mass deforms under load. Each unit deforms, and more void is occupied by solid material; air is progressively expelled, and void capacity lost as product deformation progresses. The process is said to terminate upon total loss of the available void capacity and attainment of a so called limiting deformation [1].

Depending on the nature of the compressed material and its level of moisture during densification, the process may or may not be accompanied by the expulsion of liquid fluid from the material or its voids. Where there is likelihood for such occurrence, some explanations have been put forth as touching the mechanism of release and transport of such fluid or essence. Part of such essence is chemically locked in the material at cellular level and where it is oleaginous it would be mostly held as stable small spherical subcellular bodies of sizes of the order of ≤1μm [26] and major occurrence would be in the embryo and endosperm of the cytoplasm of plant seeds although also in seed coats. Two views are advanced on the mechanical release of such essence, including cell rupture and porosity of cell walls. Flow through plasmodesmata has however been argued to be the predominant form of fluid transport in compressed materials [27]. One often neglected argument is insensible heat which arguably could account for significant demands in energy for the release of fluid essence and their transport through the porous media, in addition to the contributions of gravity and the induced pressure gradient. Determination of such energy demands would be complex.

2.4. Assessing Mechanical Response and Performance during the Densification of Agricultural Products

Indices for measuring response during the densification of biological materials may be classed under mechanical response and performance. Mechanical response of biological materials to compressive load may be perceived in terms of the amounts of deformation or induced strain. Although strain may be volumetrically determined, in constrained vessels such as is peculiar to compressive expression, this parameter equates to linear strain. The modulus of deformation comprises an elastic and inelastic component. Different forms of this index are reported in literature. Constraining however limits the dimensions in which strain and hence bulk rendition of the deformation modulus may be determined. The route for the dissipation of energy is not purely deformation. Energy is also absorbed through friction and fluid transport. Depending on the level of moisture present in the biomaterial, transported fluid may be air or its combination with some liquid essence which may result either as a desirable outcrop of the unit process or an uncontrolled accompanying outcrop. Other indices of interest include the products compressibility or the compression ratio, durability of compressed materials, bulk modulus and bulk density of the compressed material. Relaxation and creep are two other responses of densified materials which are important in evaluating the performance of any scheme and the behavior of materials.

Two types of the bulk density are mentioned in reference to the compressed material namely, the instantaneous bulk density upon compression and the relaxed bulk density. There is no uniformity in the durations considered by different authors with respect to relaxation. Available references in the treatments of densified product forms define an initial instantaneous density and relaxed density, possible after product relaxation and expansion in the unloaded state. In bulk agricultural materials, both elastic and plastic deformations occur during the process of densification [16]. Apparent elastic and bulk product moduli may be defined [23, 28]. Relaxation is responsible for equilibration of the acquired packing state. Two concepts of this are presented to wit measured relaxation after compression [29–31] and in-storage attributions to gains in size of the densified material [32]. Both of these are related to a so called initial or instantaneous density of the compressed bulk material [32, 33] and product quality measured through some test for durability [33, 34]. Most of the studies on relaxation and creep in bulk compressed materials sought to fit existing mechanistic or analytic forms to experimental data, especially for straw-based materials [22, 29]. Renditions of these behaviours in different materials have only been complex. Whereas single kernel responses have been shown to be distinct [35, 36], they offer a means for the expression of determinable bulk characteristics. For individual seeds, studies on stress and strain relationships reveal five important points, the most prominent being the bioyield point beyond which deformation is inelastic [37, 38]. In bulk materials, these points appear to be non-prominent in essentially all of the studies reported [39]. Whereas rupture stresses are described for single elemental units of agricultural materials, such descriptions are seldom done for their bulk presentations, perhaps because these regions are subsumed in responses commonly presented with high pressure treatments. Existing studies [3, 22] attest to this. Studies relating the failure of bulk plant material matrices to bioyield strengths are seldom reported. However, attempts at understanding the responses of, especially, bulk fibrous presentations are reported [25].

2.5. Parameters Influencing Densification of Agricultural Products

Several parameters influence the process and course of densification of biological materials, including process requirements such as the compression ratio, compression speed, porosity index, initial product density and the bulk compression modulus [1, 5, 40–42]. Some of these parameters have been investigated for mostly woody and fibrous agricultural materials. Physico-chemical and thermo-mechanical effects may be encountered when formulating products. Physical parameters have pronounced effects on mechanical response [43–45]; for instance, while friction lessens as densification progresses, moisture is a plasticizer and response to this factor is a complex phenomenon [6, 46]. Thermal influences result in chemical modifications which affect the behaviours of these materials [34, 47, 48].

Moisture exhibits considerable influence on different response parameters during the densification [49] and this influence is complex [46]. Products with smaller particle size tended to result in more better densification [50].

Mechnical properties influence the process of densification of agricultural products significantly. A few studies [2] detail the contributions of friction and observations were drawn as to product depth or length in the compression chamber. This effects have been quantified for crystalline materials in terms of the induced stress and the materials aspect ratio [51].

Process parameters affect the performance of densification systems and product quality [52]. Moisture is an effective plasticizer, and its level during processing lowers the glass transition temperatures [53]. Whereas feedstock moisture may lower glass transition temperatures of the processed material it results in higher moisture presence in the final product [34] with pronounced effects on other process and product properties [54]. Pressure was the most important contributor to specific energy demand compared with other system variables [42, 55].

2.6. Models of the Densification of Biomaterials

Skalweit [56] proposed a relationship of the form:

$$p = c\gamma^m \tag{2.1}$$

where, p is applied pressure and γ the current density of the material, c and m being constants. Mewe [57] expanded this relation (Eq. 2.2) to include the initial product density, γ_o so that

$$p = b(\gamma - \gamma_o)^n \tag{2.2}$$

Mewe's relationship was found to be valid at low pressures up to 1 MPa. Osobov [58] derived an exponential expression for relating the same parameters (Eq 2.3):

$$p = \frac{C}{a}\left(e^{[a(\gamma-\gamma_o)]} - 1\right) \tag{2.3}$$

For simplicity of form, and supposing that a certain speed coefficient is independent of the ratio in question, Skalweit's and Mewe's relationships for relating pressure to compressed product density were favoured over Osobov's [59].

Faborode and O'Callaghan [1] proposed an exponential model to relate the pressure acting on an elemental disc of material at a depth, *x* in a pressure vessel to the initial produce density, compression ratio, porosity index and the material's bulk modulus. Pressure was represented as:

$$P_x = \frac{K_O}{b}\left[e^{b(r-1)} - 1\right]e^{(-\mu k x)/R} \quad (2.4)$$

where, K_O is the initial bulk modulus, μ the friction coefficient and P_x the compression pressure at x. Nona et al. [4] attempted describing compression of some fibrous agricultural materials using Maxell and Peleg's constitutive models but concluded that Faborode's exponential model provides a more acceptable description of the process up to a density of 145 $kg.m^{-3}$.

Uziak [59] adopted modified forms of the power functions above to determine pressure acting on the surface of a piston acting on bulk straw material.

Skalweit's equation has been shown to relate particularly to inter-tier space filling; the filling of internal void cavities presented better as power functions [6]. However, unlike simple exponential forms [60], concepts of solid phase compression with recourse to phenomenological interpretations of the loss of void capacity were demonstrated to be relevant in predicting mechanical response in densified products, the effectiveness varying with prevailing pressure regimes [2]. Power relations were more sensitive in high pressure zones while Skalweit's model had better effect in low pressure regimes; uncertainties and variations in the effects of these models were associated with crop materials, changing physical parameters [6] and heterogeneity [7], even in zones where similarities of behaviour were expected. Whereas these models were investigated for fibrous biomaterials, it is possible to adapt them for bulk agricultural products of the nature considered in this study.

Most existing studies consider densification of bulk grain materials in whole or comminuted forms without reference to the influence of friction. Basis for inclusion of the factor in schemes where the effects may be pronounced however exist [7] particularly considering effects along the walls of the product restraining structure [61, 62]. This study seeks to understand mechanical response of selected agricultural products and their presentations and to establish forms for their prediction in under triaxially imposed stress conditions. No thermal modifications of feedstock properties are anticipated for this study. The states of stress are to be steadily induced at such rates as to exclude the occurrences of dynamic events.

2.7. Study Crops

Carob (*Ceratonia Siliqua* L.) is a perennial legume [63]. Although it has different uses such as the exploitation of its pod for animal feed, the seeds for natural gum and pulp as carbohydrate feedstock for ethanol production [64] its chief importance is as food and nutraceutical stock. Pulp or powder from the pod of carob is prized for high nutritional and medicinal value, being essentially about 76% carbohydrate, 6% protein and 2% fat; as powder, this fruit essence is a rich source of important vitamins and minerals, including iron, calcium, sodium, niacin, vitamins B6, C, D and E and an important alternative to cocoa powder and derivative products, particularly due to its low caffeine and theobromine content [65, 66]. Carob is also high in dietary fibre and phenolic compounds. Annual pod production statistics fluctuated between 158,609 t – 656,877 t at a yield rate of 2318 – 2937 $kg.ha^{-1}$ [67].

Lentil (*Lens culinaris* Medik) is equally an economically important food legume [68], with up to 2% fat and 32% protein content. The seeds also contain iron, cobalt, iodine, lysine and arginine. Lentils are 27.7% protein, 1.0% lipid, 4.1% crude fibre, 2.6% ash and 61.2% carbohydrate. They are also rich in micronutrients, including calcium, iron, zinc, thiamin, folate, and vitamins A and C. Lentils are often employed for enhancing nutritional and dietary qualities of noodles, spaghettis and pastas [69–71]. Annual production of lentils ranged between 854,877 t on 1,619,653 ha in 1961 to 6,315,858 t on 5,481,120 ha in 2016. Asia accounted for 63.8% world total production in this period while Europe accounted for 3.5% of the figure, 26.5% and 4.3% coming from America and Africa [67].

The seed of chickpea (*Cicer arietinum* L.) is, by mass, 19.5% protein, 5.7% lipid, 4.0% crude fibre, 2.7% ash and 61.7% carbohydrate. It is also rich in micronutrients, being slightly higher in calcium and folate than lentil [69–71]. Annual production of chickpeas was 7,681,851 t on 11,836,682 ha in 1961 and 12,092,950 t on 12,650,078 ha in 2016. Asia, Africa, Americas, Oceania and Europe accounted, respectively, for 88.6, 4.2, 3.5, 2.1 and 1.5% of total world production figures in this period [67].

3. Model Development and Verification

3.1. Influence Factors and Variable Groups

Three groups of variables influence mechanical response during the densification of agricultural products namely, physico-mechanical properties of crops, machine geometrical and load related factors and operational and process parameters. It is possible to establish relationships which would be useful in describing the behaviours of agricultural products under high hydrostatic pressure regimes in terms of variables belonging to these broad groups. Some of the important crop variables include product moisture content – this has effect on a product's true and initial bulk density; moisture, porosity and product density are strongly correlating parameters. Other crop factors include individual seed hardness or its strength in compression, seed-vessel friction and seed-seed friction. Machine factors include the characteristic dimension of the pressing vessel (which in this case is its diameter), depth of product fill in the compression chamber and the applied pressure. The listed geometrical parameters constitute the equipment's aspect ratio. Process variables include the time rate of deformation and temperature. The time rate of deformation is the most important determinant of the rate of induction of strain. The factors mentioned constitute a pool and only a feasible few would be selected for this study namely, applied compressive stress, p (Pa), time rate of deformation, r_d ($m.s^{-1}$), vessel diameter, D (m) and pressing depth, H (m).

3.2. Determination of Functional Forms

Functions to explain the behaviour of granular agricultural materials of the type considered in this study may be synthesised in agreement with existing works [2, 3, 6, 7] on bulk fibrous biomaterials with shared peculiarity of heterogeneity in material properties.

Blahovec [3] presented a model to express the weight-dependence of applied pressures, p in biomaterials of the form

$$p = a\rho^n \tag{3.1}$$

where, ρ is density, kg.m^{-3}, such that specific work may thereby be determined as

$$w = \int_{\rho_1}^{\rho_2} \frac{p_2}{\rho^2} d\rho \tag{3.2}$$

where, w is specific energy, J.kg^{-1}. or

$$w = \frac{a}{n-1}(\rho_2^{n-1} - \rho_1^{n-1}) \tag{3.3}$$

where, ρ_1 and ρ_2 are initial and compressed material densities. A better procedure for describing the process was developed [2] based on the concept of solid phase compression and a phenomenological description of the process of the filling of the voids and cavities, considering the contributions of friction on the wall of the pressing chamber. In the solid phase,

$$p = K \ln \frac{\rho}{\rho_s R} \tag{3.4}$$

where, $R = 1 - i$, the proportion of solids in the matrix, and may be expressed [2] as

$$R = \frac{k_1\left({}^{\rho_o}/_{\rho_s}\right) + \left({}^{p}/_{p_1}\right)^l}{1 + \left({}^{p}/_{p_1}\right)^l} \tag{3.5}$$

where, ρ_o is initial bulk density and ρ_s is bulk density of the cell wall material. A description of the process leading to the loss of porosity in a bulk material matrix with reference to pressure is only possible in terms of the induced hydrostatic pressure in the material [2].

Assuming that the loss of porosity with increasing pressure is proportional to the power of pressure and porosity - i being porosity - that is,

$$-\frac{di}{dp} = (m+1)\frac{p^m}{p_o^{m+1}} \cdot i \tag{3.6}$$

$$i = C \cdot e^{\left[-\left(\frac{p}{p_o}\right)^{m+1}\right]} \tag{3.7}$$

This is true, since porosity varies as the gradient of its loss [2].

The first phase of deformation is dominated by rearrangement of particles in the bulk material matrix to occupy available void spaces. For this response, initial bulk density of the material increases from some value ρ_o to an instantaneous value, say ρ_p. Further loss of porosity in the material leads to the acquisition of another value of density, ρ_s which is relatable to the material's cell walls, however small this may be argued to be, given the solid nature of the material. At these points, the material's porosities, i_1 and i_2 are associated with ρ_p and ρ_s, respectively. By superposition, the two partial porosities may be expressed [2] as:

$$i = i_1 + i_2 - i_1 \cdot i_2 \tag{3.8}$$

From the established exponential form,

$$i_1 = \left(1 - \frac{\rho_o}{\rho_p}\right) \cdot e^{\left[-\left({}^{p}/{}_{p_{o1}}\right)^{m_1+1}\right]} \tag{3.9}$$

p_{o1} and m_1 are parameters characterising filling in the intersticial spaces. And

$$i_2 = \left(1 - \frac{\rho_p}{\rho_s}\right) \cdot e^{\left[-\left({}^{p}/{}_{p_{o2}}\right)^{m_2+1}\right]} \tag{3.10}$$

whence, for small pressures [2], by substituting, Eq.3.8, we may obtain the form

$$\rho - \rho_o = A\left(\frac{p}{p_{o1}}\right)^n \tag{3.11}$$

where, $A = \rho_p - \rho_O$ (3.12)

and $n = 1 + m_1$ (3.13)

express the interdependencies of the function parameters.

It is preferable [2] to describe the compression of the bulk material in terms of the applied or external pressure, p', since this particular pressure acts on the entire matrix – solid material, voids and cavities.

If we assume that forces acting on the solid components of the compressed material are evenly distributed, we may [2] write an approximate relationship for the external applied pressure and the stress induced internally in the material as follows:

$$\overline{p'} = R^{2/3} \cdot \bar{p} \tag{3.14}$$

The mean piston pressure, $\overline{p'}_x$ [2] is given by

$$\overline{p'}_x(l, 0) = \frac{4 \cdot F}{\pi d^2} \tag{3.15}$$

which is independent of l, the compression ratio. However, as a result of the effects of friction along the longitudinal axis, x, this pressure decreases with distance from the piston face of the piston [2].

If we assume [2] that the distribution of pressure $\overline{p'}_x$ is uniform, radially, than we may express a lateral pressure factor, ξ as follows, $\bar{p}_T$ is the lateral pressure:

$$\xi(l, x) = \frac{\bar{p}_x(l, x)}{\bar{p}_T(l, x)} \tag{3.16}$$

The axial pressure in the compressed material may [2] be expressed as:

$$\bar{p}'_x = \frac{3}{1 + 2\xi} \cdot R^{2/3} \cdot \bar{p} \tag{3.17}$$

The lateral pressure coefficient may be expressed thus:

$$\xi = \xi_{as} R \tag{3.18}$$

The pressure differential along the longitudinal axis and resulting from the effects of friction, largely along the wall of the compression chamber causes reductions in the intensity of pressure axially, away from the face of the compression piston and may be expressed as [2]

$$d\bar{p}'_x = -\frac{4}{d}\bar{p}'_x \xi f dx \tag{3.19}$$

where, f is coefficient of friction, and

$$\bar{\rho} = \frac{1}{l}\int_0^l \rho(x)\, dx = \frac{4m}{\pi d^2 l} \tag{3.20}$$

Substituting for dx and simplifying, we obtain

$$\bar{\rho} = \frac{1}{l}\int_{\bar{p}'_x(l,0)}^{\bar{p}'_x(l,l)} \frac{d}{4\xi f} \cdot \frac{\rho(x)}{x} dx \tag{3.21}$$

We may [2] integrate the last equation to obtain a relationship for the height of compressed material with respect to the applied pressure as follows

$$l = \frac{d}{4}\int_{\bar{p}'_x(l,0)}^{\bar{p}'_x(l,l)} \frac{dx}{\xi f x} \tag{3.22}$$

These relationships are useful and may be implemented carefully to describe the behaviour of agricultural products under the influence of high hydrostatic pressures.

3.3. Techniques for Model Verification

Functional forms relating response quantiles to the compression of the selected agricultural products would be established using the models above and non-linear regression technique. This technique is well developed and properly documented [2, 72, 73] and may be implemented on many data analysis platforms.

3.4. Model Validation

The object of validation is investigating whether or not the outputs of a verified model are consistent with observations. The observations may be those of existing models or alternative means of solution or those made during investigations performed on the real system being modeled. Validation may be accomplished analyses of residuals, either by comparing differences between predictions and actual measurements or correlating model output with actual system measurements graphically. What is normally required is to establish discrepancies (or the level of such) in measurements done using the model. The root mean square of deviation and correlation coefficient are two useful statistics in this regard [73]. Other fitting measures evaluating bias, dispersion and the prediction mean of square may also be readily sourced from literature where they are applicable.

4. Materials and Methods

4.1. Materials

Three crops were suggested for this study, namely *Ceratonia siliqua L., Lens culinaris Medik. and Cicer arietinum L*. These crops are important food, feed and nutraceutical crops. The batches of the crops used for the study were sourced from the Czech Republic. Grains were cleaned prior to their use. Powder forms of *Lens culinaris Medik. and Cicer arietinum L* were obtained through careful milling in a laboratory impact mill using 1 mm screens.

4.2. Equipment Description and Working Principles

Basic outlay of the experimental setup is described in literature [7] and is shown in Figure 4.1. The test rig consisted of a high pressure product compression device, a load source and data acquisition systems. The compression device consisted of a cylindrical steel pressing vessel of with an internal bore diameter of 25 mm with and a wall thickness of about 40 mm. The vessel was provided with a 100 mm thick circular base plug stepped inwards diametrically at 25 mm depth from its top, 37.5 mm from its circumference. The plug is positioned concentrically in a cylindrical support which is fitted on its exterior with strain gauges for friction measurement. A thin sheet separates the plug from the support ring. The ring sits on the cross-head of the load source, positioned on a 25 mm thick circular steel base; the pressing vessel rests on the cylindrical support. A solid steel piston of uniform diameter (of 25 mm) fitting closely in the bore of the vessel is loaded axially through a hemispherical disc such that it constitutes the moving member while the base plug remains relatively fixed. The piston has a flat base.

The assembled device was mounted on the bed of a Tempos ZDM 50 model universal test rig manufactured by Tempos s.r.o of Czech Republic and loaded compressively through a hemispherical disc at the head of the piston. The mobile element of the rig was the load bed or cross-head. The equipment was engaged at about 5 $mm.min^{-1}$ with a load of 20 N. Once engaged, the motion of the cross-head was discontinued and the programmed test settings defaulted to at the commencement of the test.

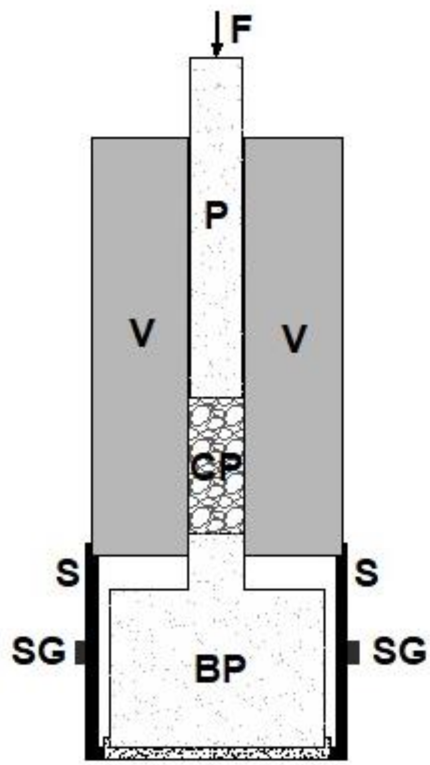

Fig. 4.1. The product compression scheme showing the piston (P), pressing vessel (V), compressed material (CP), base plug (BP), support ring (S), strain gauge (SG) output nodes, and applied compressive load (F)

All tests were conducted under laboratory condition of 20°C. Uniform replicated bulk volumes of materials would be used and in reference to test treatment levels. Products were fed into the compression vessel under gravity, in free fill to desired test depths. This was done prior to the installation of the piston. Subsequently, the filled vessels with piston in place were mounted on the bed of the rig and the bulk material gradually loaded from 0 N to peak test load corresponding to the compressive stresses of interest at the selected cross-head velocity. Upon attaining the desired peak value, the application of load was discontinued and the device unloaded. Necessary ancillary parameters were then acquired.

4.3. Instrumentation and Measurements

Compression load was applied via a Czech model universal test rig, the ZDM50; it is a product of the old Czechoslovakia and was modernised by Tempos®. Compression test data were acquired from this machine electronically using the TIRAtest software developed by TIRA GmbH of Germany.

Frictional loads during densification were measured using special instrumentation consisting of strain gauges mounted on some base support for the compression device. The design is such that reaction load for compression force is supplied through a base plug whose smaller end fits in the die and whose base rests on a base but with a circumferential clearance of about 3mm from the load sensing arms of a cylindrical support upon which rests the pressure vessel; vertical deflections in the load sensing arms are processed for the contributory effects of friction along the internal wall of the die, at its interface with the compressed material matrix. A schematic illustration of the arrangement is shown as Fig. 4.1. Stripped components of the friction data acquisition units are shown as Appendix C. The support unit is the cylindrical steel support with four slender bars, which is fitted with strain gauges as shown. Net deflections in these bars during compression are as a result of frictional drag on the internal walls of the die. The signal is sensed and communicated to a data acquisition unit which is connected to a PC. The unit is operated by a data acquisition software developed at the Faculty of Engineering of the Czech University of Life Sciences. Friction test data were therefore electronically logged. The friction test device was calibrated prior to use on a separate universal test rig other than the one used for the experiments documented in this report. The calibration chart is shown as Appendix B. Upon assembly, the compression and friction test device are mounted on the ZDM50 universal test rig, as shown in Plate 4.1. For whole seeds, moisture measurements were done using the oven drying method in accordance with the ASAE standards S352.2 [74] for moisture determination in unground grains and seeds. Each 15 g sample was oven dried in a Gallenkamp Memmert type hot air oven at 103±2°C. The masses of the samples used in the course of the study were weighed using the Kern 440–35N (Kern & Sohn GmbH, Stuttgart, Germany) top loading type weighing balance. Moisture determination for the food powders was in accordance with the ISO 712:2009 [75] routine reference method for the determination of moisture contents of cereals and cereal products; approximately 5 g samples were oven dried at 130±3°C for an initial 2 hours, and a subsequent 1 hour, where required.

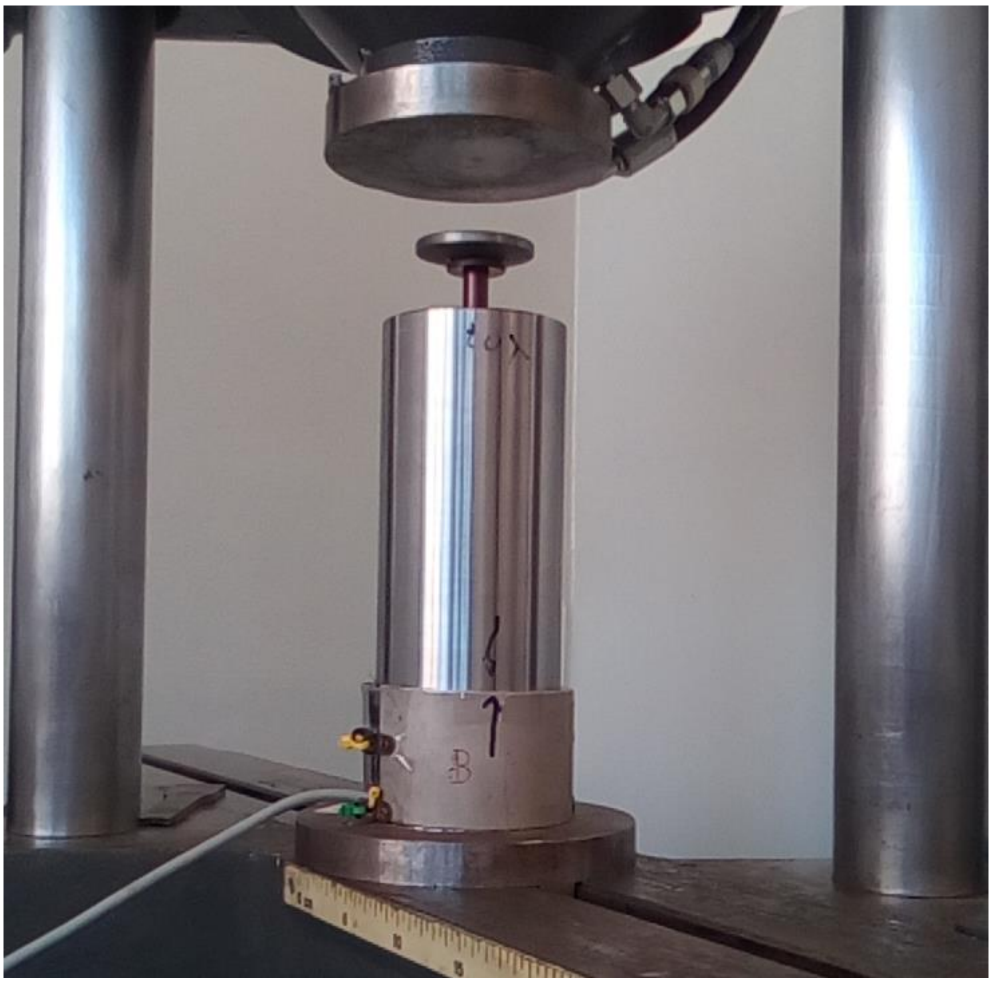

Plate 4.1. Assembled compression and friction test device

True densities of all seeds and powders reported in this study were obtained using the micrometrics® AccuPycII 1340 model gas displacement pycnometer (Plate 4.2), manufactured by Micromeritics Instruments Corporation, Norcross, Georgia, USA. The basic principles of the operation of the equipment are described in literature [76, 77]. The equipment is run on a data acquisition software, developed by the same company.

Plate 4.2. True density measurement system

For food powders, it is necessary to specify their volumetric weights in terms of the methods of their acquisition, since each parameter defines a unique condition of the test material. Bulk densities are acquired as free-fill, mass-volume relationships and represent a measure of the bulk weight of the material howbeit with all the interlocked air, voids and spaces. Tapped densities refer to bulk material densities acquired by inducing particulate settlement through gentle re-organisation of the component materials and the gradual elimination of void. The results depend on the extent of induction of this settling through 'tapping'. Tapping is done using a special configuration of devices of the form illustrated in Fig. 4.2. The approach may vary in certain cases but the principles are the same. Food powder is fed into a cylinder (often of steel) of about 250 ml capacity, designed to sit in the holder of the tapped density device. A vertical shaft is made to induce and sustain the vertical oscillation of the cylinder such that the resulting impact is of the weight of the sample power itself. Oscillation is delivered via an eccentric drive which runs at about 250 rpm, with an eccentricity of 3±0.2 mm. The relevant standards [78] require that 10, 500 and 1250 taps be separately but progressively implemented on the same powder sample until not more than 2mm settlement is recorded between the last tap at 1250 and test preceding it. Detailed description of the procedure may be found in reference sources [78–80]. These tests were conducted for the powders of chickpea, lentils and carob, according to the ASTM D7481-18 Standard test methods for determining loose and tapped bulk densities of powders using a graduated cylinder (Fig. 4.2).

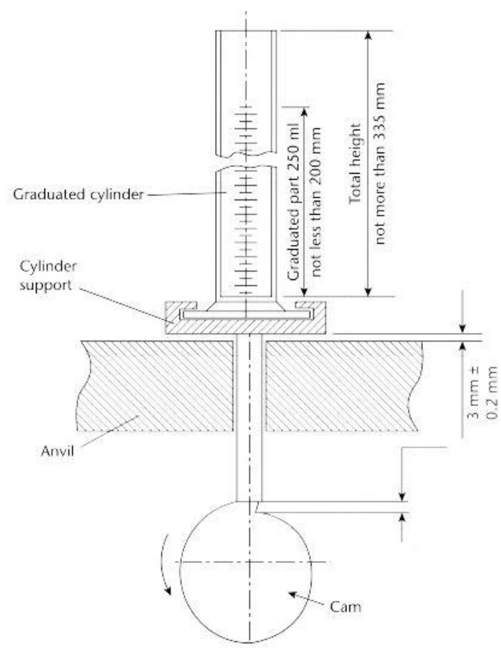

Fig. 4.2. Basic approach to the acquisition of tapped density of food and related powders
Source: USPC [80], WHO [79], ASTM [78]

4.4. Ancillary and Response Parameters and Procedures for their Determination

Osobov [58] describes the compression of a material within a die; and illustration of an elemental disc of material within the compressed matrix is shown in Figure 4.3. The following parameters may be defined:

p – applied pressure on the face of an elemental disc of material at a distance x from the face of the piston

dx – the thickness of the elemental disc of material

a – cross-sectional area of the compressed disc, perpendicular to the direction of the applied pressure

p_s – radially acting lateral or side pressure, acting on the wall of the die

τ – shear resistance along the interface between the compressed material and the die wall. The force responsible for this is assumed to be purely due to friction along the material-wall interface. The effect of rolling friction is not considered, as also the forces of adhesion between the material and the wall during compression.

μ – coefficient of wall friction; this is the coefficient of kinetic friction

F, F_S and F_t – applied normal, lateral and friction forces, respectively

D – diameter of the die or characteristic dimension of the compression vessel

u – surface area of the elemental disc of the material in contact with the wall of the die

Axial, radial and shear stresses acting on the elemental disc, and the respective forces, are indicated in Figure 4.3.

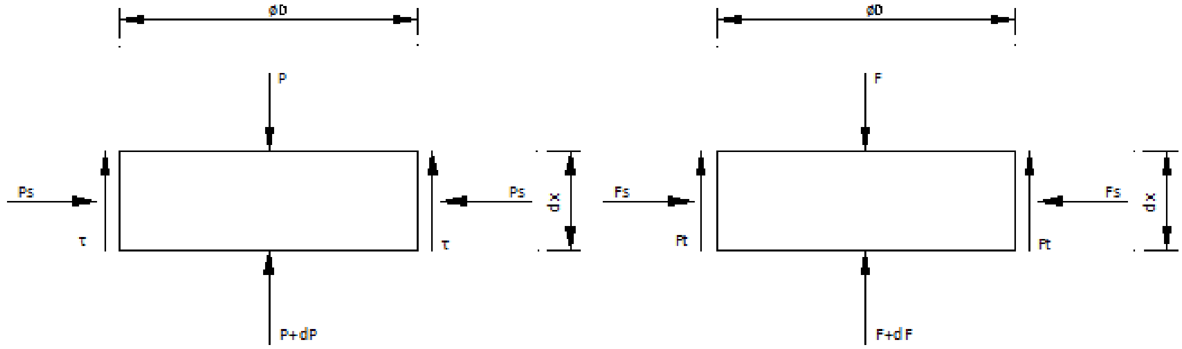

Fig. 4.3. Forces acting on an elemental disc of material within the compressed material matrix

$$dF = -F_t \qquad (4.1)$$

where, dF is elemental force, N and F_t is frictional drag, N

$$F_t = \mu F_s \qquad (4.2)$$

where, F_s is radial force, N and is μ friction coefficient, -, at the material-wall interface

$$p_s = \xi p \qquad (4.3)$$

where, p_s is lateral or side pressure, Pa, ξ is the pressure ratio, - and p is applied axial pressure, Pa

$$F_s = p_s . u \qquad (4.4)$$

where, u is wall contact area, m^2

$$F_S = \xi p . u \qquad (4.5)$$

$$F_t = \mu F_s \qquad (4.6)$$

$$F_t = \mu \xi p . u \qquad (4.7)$$

$$p = \frac{F}{a} \tag{4.8}$$

where, a is projected area of the disc normal to the applied axial force, F

So that

$$dF = -\mu\xi \frac{F}{a}.u \tag{4.9}$$

$$u = \pi D.dx\ ; \quad a = \frac{\pi D^2}{4}\ ; \qquad \frac{u}{a} = \frac{4}{D}dx$$

and, where D is the diameter of the elemental disc,

$$dF = -\mu\xi F.\frac{4}{D}dx \tag{4.10}$$

$$\frac{dF}{F} = -\frac{4\mu\xi}{D}dx \tag{4.11}$$

For initial and final piston face positions 0 and 1, respectively, the effective forces are F_0 and F_1, the original depth of the product bed being H_0.

At F_1, therefore,

$$\int_{F_0}^{F_1} \frac{dF}{F} = -\frac{4\mu}{D}\int_0^H \xi dx \tag{4.12}$$

$$ln\left(\frac{F_0}{F_1}\right) = -\frac{4\mu\xi}{D}(0 - H) \tag{4.13}$$

$$\mu\xi = \frac{D}{4H} ln\left(\frac{F_0}{F_1}\right) \tag{4.14}$$

$$F_1 = F_0 - F_t \tag{4.15}$$

$$H = H_0 - \delta \tag{4.16}$$

where, $\delta =$ deformation

So that,

$$\mu\xi = \frac{D}{4(H_0 - \delta)} \ln\left(\frac{F_0}{F_0 - F_t}\right) \tag{4.17}$$

$\mu\xi$ is the side pressure factor, a product of the wall friction coefficient, μ and the pressure ratio, ξ. The pressure ratio is the ratio of the radial or side pressure, p_s to the applied axial pressure, $\bar{p}$.

$$\mu\xi = \frac{p_s}{\bar{p}} \tag{4.18}$$

Where the coefficient of wall friction is established, the mean pressure acting on the wall of the compression vessel, $\bar{p}_s$ may be evaluated, for elemental sections, as

$$\bar{p}_s = \frac{D \ln\left(\frac{F_0 - F_t}{F_0}\right)}{4\mu H} \bar{p} \tag{4.19}$$

where, $\bar{p}$ is the mean applied pressure.

The wall friction coefficient may be determined for different agricultural products and the material of the internal wall of the compression vessel through separate experiments as the kinetic friction coefficient, since this is the predominant friction during quasi-static compression of bulk materials in constrained configurations of the type discussed in this study, such that,

$$\mu = \mu_w = \mu_k \tag{4.20}$$

where, μ, μ_w and μ_k are symbols denoting friction coefficient, coefficient of wall friction and coefficient of kinetic friction, respectively.

The ratio of the force of friction to the applied compressive force may be determined using Eq. 4.21:

$$r_f = \frac{F_t}{F} \tag{4.21}$$

where, r_f is the friction ratio, -, F_t is the force of friction, N measured using strain gauges, F and is the applied compression force, N.

Procedures for the determination of the physical parameters of interest are described in literature [81, 82]. Mechanical response and performance indicators may be established using ancillary characters logged during each test [7]. Induced strain may be determined as the ratio of the peak deformation during a test to the initial product depth established prior to the commencement of that test. Energy requirement may be established for a given load and the attending deformation. Effectively, this energy must be evaluated as a function of the attending frictional energy demand [83]. Specific mechanical energy is energy per unit volume of compressed material [84]. For any treatment combination, this may be expressed as the ratio of the deformation energy to the initial volume of the material compressed during each test. The modulus of deformation of the compressed bulk material may be determined as the slope of the stress and strain or deformation curve at the specified force.

The highest value of deformation which obtains in the compressed material at peak load is δ_c (mm). The initial depth of the bulk material in the compression chamber is H_o (mm). Strain induced in the compressed material ϵ (-) may be computed using Eq. 4.22.

$$\epsilon = \frac{\delta_c}{H_o} \tag{4.22}$$

The rate of strain, $\dot{\epsilon}$ may be determined as a function of the time to deformation, t_c given the applied compressive force and the prevalent equipment and process conditions Eq. 4.23:

$$\dot{\epsilon} = \frac{\epsilon}{t_c} \tag{4.23}$$

The initial volume of compressed material, V (mm^3) may be evaluated using Eq. 4.24:

$$V = \frac{\pi D^2}{4} \times H_o \tag{4.24}$$

where, D (mm) is the internal diameter of the cylindrical compression vessel.

The initial bulk density of the uncompressed material was determined as the ratio of the mass of a sample of the agricultural product, m (g), as treated, to its known free–fill volume, V_{ff} (mm^3). This may be expressed as shown in Eq. 4.25 below:

$$\rho_b = \frac{m}{V_{ff}} \tag{4.25}$$

The initial porosity, P_f (%) or void capacity of a batch of agricultural product may be calculated using Eq. 4.26 [81, 82]:

$$P_f = \left(1 - \frac{\rho_b}{\rho_t}\right) \times 100 \tag{4.26}$$

where ρ_b ($kg.m^{-3}$) and ρ_t ($kg.m^{-3}$) are the bulk and true densities of the product, respectively.

Bulk density of the compressed material, ρ_c ($kg.m^{-3}$) was determined as a function of the mass of the compressed material, m_c (g) and its final volume, V_c (mm^3) after compression (Eq. 4.27).

$$\rho_c = \frac{m_c}{V_c} \tag{4.27}$$

and

$$V_c = \frac{\pi D^2}{4} \times (H_o - \delta_c) \tag{4.28}$$

The effective applied pressure, p_a (Fig. 4.3) may be expressed as:

$$p_a = 4 \cdot \frac{F - F_t}{\pi d^2} \tag{4.29}$$

where, F_t is measured with a strain gauge, arising from friction between the piston and the wall of the compression chamber and between the compressed material and the wall of the compression chamber.

Deformation energy is the energy required to compress the biomaterial and may be determined as the area beneath the force deformation profile of the compressed material. It is the energy required to achieve a given deformation of the compressed product mass, at the specified force and conditions. This may be computed through numerical integration using the trapezoidal rule (Eq. 4.30) [85]:

$$E_v = \sum_{n=0}^{n=i-1} \left(\frac{F_{n+1} + F_n}{2}\right)(\delta_{n+1} - \delta_n) \quad (4.30)$$

where, i represents the number of subdivisions of the deformation axis, F_n (N) being the compressive force for a known deformation, δ_n (mm) and E_v (J) the deformation energy; F is net force acting on the material for its densification, subtracting the effect of friction. Volume specific energy demand, $\dot{E}$ (J.mm^{-3}) may be calculated as the ratio of the deformation energy to the volume of the deformed material (Eq. 4.31).

$$\dot{E} = \frac{E_v}{V} \quad (4.31)$$

Specific energy may be alternatively computed through the same numerical computation procedure using Eq. 4.32.

$$\overline{\omega}_{\bar{\rho}} = \int_{\rho_1}^{\rho_2} \frac{p_2}{\rho^2} d\rho \quad (4.32)$$

where, $\overline{\omega}_{\bar{\rho}}$ is mass specific energy requirement, J.kg^{-1} for achieving a given deformation in consonance with an attained density ρ_2, kg.m^{-3}, given an initial product density, ρ_1, kg.m^{-3} and an applied pressure, p_2, Pa. It's time rate of expenditure may then be obtained as a function of the time taken to compress the material and may thus be regarded as specific power (in W.kg^{-1}) (Eq. 4.33):

$$\dot{\bar{\omega}}_\rho = \frac{\overline{\omega}_{\bar{\rho}}}{t_c} \tag{4.33}$$

where, $\dot{\bar{\omega}}_\rho$ is specific power, W.kg^{-1}, and t_c is time to compression, *s*.

Gain in bulk density by the product may be determined using equation 4.34:

$$G_\rho = \left(\frac{\rho_c}{\rho_o} - 1\right) \times 100 \tag{4.33}$$

where, G_ρ is gain in bulk density, %, ρ_o is initial bulk density of the material before compression, kg.m^{-3} and ρ_c is bulk density of the compressed material, kg.m-3,

The aspect ratio, r_a, - is the ratio of the depth of product charge, H, mm to the characteristic dimension of the compression vessel (Eq. 4.34). For a cylindrical cross-section, this dimension is the internal diameter *D*, mm of the compression vessel.

$$r_a = \frac{H}{D} \tag{4.34}$$

The time rate of deformation, r_d, mm.s^{-1} is the ratio of achievable deformation, δ_c, mm to the time to deformation, t_c, *s*. (Eq. 4.35):

$$r_d = \frac{\delta_c}{t_c} \tag{4.35}$$

This may be set on the test rig in preferred unit. The most common usage in literature is the mm.min^{-1}.

4.5. Design of Experiments

Factorial concepts were applied to the development of the relevant treatment levels. Careful considerations were given to factor level selections, as applicable to requirements for their transformations into orthogonal domains where necessary. Data for modelling mechanical response in high pressure regime were obtained for whole seed and powder forms of *Lens culinaris Medik. and Cicer arietinum L*. at ten levels of axially applied pressure in increments of 50 MPa from a minimum level of 50 MPa. Tests for each product form were conducted in three replications at similar rates of deformation as equipment aspect ratio of 5.5 $mm.min^{-1}$ and 0.5, respectively. Thirty data points were thus obtained to describe each product's compression profile and a total of 120 data points were employed for the four products. Due to the pronounced effects of stick and slip, and high friction loads observed during tests with *Ceratonia siliqua L.,* only tests describing the behaviour of this product at two base pressure levels were possible, at three rates of product deformation and three aspect ratios, or 18 treatment levels. The tests for this product were also conducted in three repeatitions and amounted to 54 experimental runs. All tests were conducted at singular storage moisture levels and laboratory conditions of 20°C and 45% relative humidity. The tests were full factorial experiments, fitted into completely randomised designs.

4.6. Data Analysis

A programme was written and implemented in FORTRAN for the computation of the relevant response parameters from the logged test data from two separate systems, namely the TIRA test programme for the time, force and deformation data and the friction test software for time and friction force data; other ancillary data such as product masses were logged manually as acquired during experiments. All reported test data were subjected to analyses of variance using Genstat*TM*. Treatment means were compared using Duncan's multiple range test. Standard statistical techniques applied to the estimation, verification and validation of the fitted functional forms, including methods for the analyses of residuals, are properly discussed in literature [73, 86]. Model parameters were generated using TIBCO®'s STATISTICA*TM*, version 13. Characteristic densities of the various products were determined using Mathematica*TM*. Other computations were done using MS Excel.

5. Results and Discussion

5.1. Physico-Mechanical Properties of *Ceratonia siliqua L., Lens culinaris Medik. and Cicer arietinum L*. Relevant to their Compression

Physical properties of the test products relevant to compression are presented in Tables 5.1 – 5.4. Free fill bulk density of chickpea and lentil seeds ranged between 806.7 kg.m^{-3} – 842.3 kg.m^{-3} and 784.3 kg.m^{-3} – 851.2 kg.m^{-3}, respectively. Compared to their true densities, the bulk samples of the seeds had porosities in the regions of 39.40% – 41.96%, for chickpea seeds and and 40.35% – 45.03% for lentil seeds. The true densities of these crops were 804 kg.m^{-3} and 795 kg.m^{-3}, respectively. These values are for dry basis moisture contents of 10.8% and 11.02% for chickpea and lentils, respectively. Seed bulk densities are those obtained under conditions of free fill [87].

For powders, it is important to provide information on their true, tapped and free-fill (bulk) densities. Chickpea flour had a mean true density of 1425.8 kg.m^{-3} while lentil flour had an average true density of 1444.7 kg.m^{-3}, at 12.6% and 11.8% dry basis moisture contents, respectively. True densities of the two food powders were significantly higher than true and free fill bulk densities of whole seeds (Table 5.1). Porosity was also lower in the seeds, compared to the flours (Table 5.1). Both the index of compressibility and Hausner ratio (Table 5.2) provide indications of the tendencies of the food powders to flow or deform under load. From Table 5.2, judging from their indices of compressibility and Hausner ratios, and comparing with reference standards [88], lentil flour has fair flowability, while the flowability of chickpea is passable; carob powder has a poor tendency to flow.

Static and dynamic coefficients of friction of chickpea and lentil seeds and powders are presented in Table 5.3. The results were obtained under four similar varying normal forces of 7.62 kN, 26.95 kN, 46.22 kN and 65.54 kN. As expected, the coefficients of static friction, obtained at the threshold of motion, were higher than the coefficients of kinetic friction. During quasi- static uniaxial compression, both effects are experienced along the interface

Table 5.1. Physical Properties of the test products

Product	Moisture content (%)*	True density (kg.m^{-3})	Bulk density (kg.m^{-3}) Mass of sample (g)	Volume of free fill cylinder (ml)	Bulk density (kg.m^{-3})	Tapped density (kg.m^{-3}) ρ_{t10}	ρ_{t50}	ρ_{t1250}	Porosity (%)
Chickpea seeds	10.78±0.02	1390.00±1.00	292.40±2.70	352	830.6±7.7	-	-	-	40.24±0.55
Lentil seeds	12.62±0.28	1426.90±0.90	293.60±5.00	352	834.1±14.2	-	-	-	41.54±1.00
Chickpea flour	12.64±0.13	1425.80±1.15	44.09±1.35	74	595.8±18.3	667.12±39.22	760.15±22.25	768.18±26.38	57.49±0.37
Lentil flour	11.81±0.01	1444.70±0.35	54.03±1.47	74	730.1±19.9	794.48±33.99	836.71±23.41	851.87±40.28	49.46±1.38
Carob flour	4.51±0.02	1526.40±1.10	30.38±0.16	74	410.5±2.2	432.26±1.27	572.59±0.13	577.74±3.24	73.19±0.37

Table 5.2. Settling properties of the food flours

Product	Moisture content (%)*	Compressibility index (%)	Hausner ratio
Chickpea flour	12.64±0.13	21.04±3.41	1.27±0.05
Lentil flour	11.81±0.01	16.38±5.94	1.20±0.09
Carob flour	4.51±0.02	29.16±0.38	1.41±0.01

Table 5.3. Parameters of the coefficient of friction for four products under varying normal forces

Product	Extension (mm)	Applied Normal Force (kN)	Test speed (mm.min^{-1})	Moisture content (%)*	Maximum force (N)	Coefficient of static friction, μ_s $(-)$	Mean force (N)	Coefficient of kinetic friction, μ_k $(-)$
Chickpea flour	35.0±0.0	7.624	30	12.64±0.13	2.92±0.12	0.384±0.016	2.44±0.15	0.320±0.019
	35.0±0.0	26.95	30	12.64±0.13	8.66±0.44	0.322±0.016	7.11±0.35	0.264±0.013
	35.0±0.0	46.217	30	12.64±0.13	13.21±2.16	0.286±0.047	11.85±0.77	0.257±0.016
	35.0±0.0	65.542	30	12.64±0.13	19.27±0.81	0.294±0.013	16.96±0.28	0.259±0.004
Chickpea seeds	55.0±0.0	7.624	30	10.78±0.02	1.85±0.07	0.242±0.008	1.62±0.02	0.213±0.002
	55.0±0.0	26.95	30	10.78±0.02	6.08±0.19	0.226±0.007	5.54±0.04	0.206±0.001
	55.0±0.0	46.217	30	10.78±0.02	10.43±0.37	0.226±0.008	9.51±0.07	0.206±0.001
	55.0±0.0	65.542	30	10.78±0.02	15.13±0.19	0.233±0.003	13.54±0.06	0.209±0.001
Lentil flour	58.5±4.9	7.624	30	11.81±0.01	3.1±0.18	0.407±0.023	2.76±0.00	0.362±0.000
	43.5±16.3	26.95	30	11.81±0.01	7.41±0.17	0.275±0.006	6.90±0.04	0.256±0.001
	43.5±16.3	46.217	30	11.81±0.01	13.26±0.16	0.287±0.004	11.53±0.05	0.250±0.001
	43.5±16.3	65.542	30	11.81±0.01	17.49±0.93	0.267±0.014	14.98±0.18	0.229±0.003
Lentil seeds	55.0±0.0	7.624	30	12.62±0.28	1.67±0.07	0.219±0.009	1.52±0.01	0.200±0.001
	55.0±0.0	26.95	30	12.62±0.28	5.42±0.10	0.201±0.004	5.02±0.13	0.187±0.005
	55.0±0.0	46.217	30	12.62±0.28	9.51±0.47	0.206±0.011	8.58±0.13	0.186±0.003
	55.0±0.0	65.542	30	12.62±0.28	13.23±1.32	0.202±0.02	11.91±0.55	0.182±0.008

Table 5.4. Mean values of static and dynamic coefficients of friction

Material	Moisture content, % (dry basis)	Coefficient of static friction, μ_s (-)	Coefficient of kinetic friction, μ_k (-)
Chickpea Flour	12.64±0.13	0.321±0.046	0.275±0.030
Cheakpea seeds	10.78±0.02	0.232±0.009	0.208±0.003
Lentil flour	11.81±0.01	0.309±0.062	0.274±0.055
Lentil seeds	12.62±0.28	0.207±0.012	0.189±0.008

of the compressed product and the die wall. The coefficient of kinetic friction governs during compression when deformation of the food particulate has commenced. Static coefficients of friction ranged between 0.286 – 0.384 and 0.267 – 0.407 for chickpea and lentil flours, and 0.226 – 0.242 and 0.201 – 0.219 for chickpea and lentil seeds, respectively. The coefficient of static friction was lower in seeds than in their powders. This means that the effects of static friction along the wall of the pressure vessel are likely to be more pronounced with seeds than with their flours. A similar trend was observed with the coefficients of kinetic friction which ranged between 0.257 – 0.320 and 0.229 – 0.362 for chickpea and lentil flours, and 0.206 – 0.213 and 0.182 – 0.200 for chickpea and lentil seeds, respectively, being lower for seeds than for flours. For each product, friction parameters varied only slightly and appear to agree with available reported values [89, 90]. It is agreed that the velocity of motion seldom has significant influence on the magnitude of the kinetic coefficient of friction. As such, the average values of the coefficient of kinetic friction were used – along with other parameters – for the estimation of mean pressure acting on the die wall during compression. Pooled mean values of the coefficients of static and kinetic friction are presented in Table 5.4.

5.2. Mechanical Behaviour of *Lens culinaris Medik. and Cicer arietinum L*. during Compression

The effects of pressure, product form and their interactions on mechanical response in chickpea and lentils exposed to high axial compressive pressure in the region of 50 – 500 MPa at a deformation rate of 5.5 mm.min^{-1} and aspect ratio of 0.5 and product moisture contents of ≈ 12% (in dry basis) for chickpea and lentils within a cylindrical radial constraint of 25 mm diameter of special tool steel material are presented in Table 5.5. Both product form and applied pressure, as well as their interactions, had highly significant effects ($P<0.001$) on product compression, except for effects of pressure on the rate of strain ($P=0.995$) and of the interactions of product form and pressure ($P=1.000$) on the rate of strain and the time to peak compression, at the applied pressure. These effects are associated since indeed the rate of strain is a function of time.

Table 5.5. Effects of product forms and applied axial pressure on densification parameters

	Source of variation		
Parameter	$product$	$pressure$	$product \times pressure$
Strain, ϵ	0.001**	0.001**	1.000^{ns}
Strain rate, $\dot{\in}$	0.016**	0.995^{ns}	1.000^{ns}
Bulk density of compressed material, ρ_C	0.001**	0.001**	0.901^{ns}
Gain in bulk density, G_ρ	0.001**	0.001**	0.001**
Time, t_c	0.001**	0.001**	1.000^{ns}
Friction force ratio, r_f	0.001**	0.001**	0.001**
Pressure ratio factor, $\mu\xi$	0.001**	0.001**	0.001**
Pressure ratio, ξ	0.001**	0.001**	0.001**
Radial or lateral pressure, $\bar{p}_s$	0.001**	0.001**	0.001**
Specific energy, $\omega_{\bar{p}}$	0.001**	0.001**	0.001**
Specific power, $\dot{\omega}_{\bar{p}}$	0.001**	0.001**	0.005**

ns = not significant at the 5% level; * = significant (at the 5% level); ** = highly significant (at the 1% level).

When treatment means were compared for the different product forms, using Duncan's multiple range test, less strain was observed in product flours, compared to whole seed forms. Strain in flours ranged between 0.3203 – 0.50538 for chickpea and 0.3243 – 0.5224 for lentils, increasing as pressure increased. Between crops, strain was significantly higher in lentil flour (0.4430) than in chickpea flour (0.4277). A reversed trend presented with whole seeds as average strain in chickpea seeds (0.6660), across pressures, was higher than that recorded in whole lentil seeds, that is 0.5635 (Table 5.6).

Mean strain for all products improved with intensity of the applied pressure, being significantly higher at every level of pressure (Table 5.7) and rising between 0.4145 and

Table 5.6. Densification parameters for different product forms

Variable	Chickpea		Lentils	
	Flour	Whole seeds	Flour	Whole seeds
Strain, ϵ (-)	0.428[d]	0.666[a]	0.443[c]	0.563[b]
Strain rate, $\dot{\in} \times 10^3$ (-)	7.31[a]	7.32[b]	7.32[b]	7.32[b]
Bulk density of compressed material, $\rho_C\ (kg.m^{-3})$	1532.1[c]	2019.9[a]	1588.4[c]	1925.3[b]
Gain in bulk density, G_ρ (%)	76.58[c]	207.20[a]	81.39[c]	132.60[b]
Time, t_c (S)	58.48[d]	90.97[a]	60.52[c]	76.96[b]
Friction force ratio, r_f (-)	0.02630[d]	0.04745a	0.03787c	0.04285[b]
Lateral pressure factor, $\mu\xi$ (-)	0.01335[d]	0.02438[a]	0.01932[c]	0.02190[b]
Pressure ratio, ξ (-)	0.04855[c]	0.11720[a]	0.07051[b]	0.11590[a]
Radial or lateral pressure, $\bar{p}_s$ *(MPa)*	10.83[d]	26.81[b]	17.44[c]	32.71[a]
Specific energy, $\omega_{\bar{p}}\ (kJ.kg^{-1})$	24.70[d]	35.35[a]	26.51[c]	27.54[b]
Specific power, $\dot{\omega}_{\bar{p}}\ (W.kg^{-1})$	397.54[b]	373.18[c]	411.91[a]	341.71[d]

Mean values are compared row-wise. Similar alphabets indicate homogeneous subsets. Significant effects are valid at the 5% level of significance

0.6026.

The rate of strain varied only very slightly between product forms and was uniform across products, at all levels of pressure (Table 5.6 and Table 5.7).

Upon compression, higher bulk densities were attained by bulk seeds of chickpea and lentils (2019.9 kg.m^{-3} and 1925.3 kg.m^{-3}, respectively) than were achieved with chickpea and lentil flours which acquired mean bulk densities of 1532.1 kg.m^{-3} and 1588.4 kg.m^{-3}, respectively, upon compression. Bulk densities of compressed materials were between 1476.7 kg.m^{-3} – 1960.4 kg.m^{-3} and 1528.2 kg.m^{-3} – 2298.3 kg.m^{-3} for chickpea and lentil seeds and between 1277.6 kg.m^{-3} – 1757.9 kg.m^{-3} and 1295.2 kg.m^{-3} – 1833.4 kg/m3 for chickpea and lentil flours, respectively. Gains in bulk density were correspondingly 207.2% and 132.6% for bulk chickpea and lentil seeds and 76.58% and 81.39% for chickpea and lentil flours, respectively. This implies that more deformation occurred in chickpea seeds than in lentil seeds, per magnitude of applied pressure. The trend was reversed when the products were converted into their flours; more deformation was achieved in lentil flours per magnitude of applied

Table 5.7. Effect of pressure on densification parameters

	Applied pressure, p (MPa)									
	50	100	150	200	250	300	350	400	450	500
Strain, ϵ (-)	0.41453^{i}	0.46233^{h}	0.48753^{g}	0.50667^{f}	0.52400^{ef}	0.54020^{de}	0.55580^{cd}	0.57107^{bc}	0.58567^{ab}	0.60260^{a}
Strain rate, $\dot{\in} \times 10^3$ (-)	0.00732^{a}	0.00732^{a}	0.00732^{a}	0.00732^{a}	0.00732^{a}	0.00732^{a}	0.00732^{a}	0.00732^{a}	0.00732^{a}	0.00732^{a}
Bulk density of compressed material, ρ_C (kgm^{-3})	1394.4^{j}	1524.1^{i}	1603.5^{h}	1669.5^{g}	1734.4^{f}	1800.0^{e}	1868.5^{d}	1941.1^{c}	2016.5^{b}	2112.3^{a}
Gain in bulk density, G_ρ (%)	76.10^{j}	92.86^{i}	103.17^{h}	111.75^{g}	120.18^{f}	128.73^{e}	137.69^{d}	147.18^{c}	157.08^{b}	169.74^{a}
Time, t_c (S)	56.65^{i}	63.19^{h}	66.61^{g}	69.22^{f}	71.59e^{f}	73.80d^{e}	75.92^{cd}	78.00^{bc}	80.02^{ab}	82.32^{a}
Friction force ratio, r_f (-)	0.0488^{a}	0.0498^{a}	0.0481^{a}	0.0433^{b}	0.0388^{c}	0.0352^{d}	0.0326^{de}	0.0309^{ef}	0.0298^{ef}	0.0290^{f}
Lateral pressure factor, $\mu\xi$ (-)	0.0250^{a}	0.0256^{a}	0.0247^{a}	0.0222^{b}	0.0198^{c}	0.0179^{cd}	0.0166^{de}	0.0157^{e}	0.0151^{e}	0.0147^{e}
Pressure ratio, ξ (-)	0.1089^{a}	0.1118^{a}	0.1090^{a}	0.0990^{b}	0.0892^{c}	0.0809^{cd}	0.0751^{de}	0.0712^{e}	0.0685e	0.0669^{e}
Radial or lateral pressure, $\bar{p}_s$ (MPa)	5.46^{i}	11.23^{h}	16.42^{g}	19.82^{f}	22.37^{e}	24.32d^{e}	26.30^{cd}	28.54^{c}	30.95^{b}	34.08^{a}
Specific energy, $\omega_{\bar{p}}$ $(kJ.kg^{-1})$	5.5481^{j}	9.8328^{i}	13.762^{h}	17.97^{g}	22.866^{f}	28.468^{e}	34.841^{d}	42.041^{c}	49.847^{b}	60.075^{a}
Specific power, $\dot{\omega}_{\bar{p}}$ $(W.kg^{-1})$	97.94^{j}	156.87^{i}	208.58^{h}	262.30^{g}	322.85^{f}	389.95^{e}	463.67^{d}	544.28^{c}	628.59^{b}	735.81^{a}

Mean values are compared row-wise. Similar alphabets indicate homogeneous subsets. Significant effects are valid at the 5% level of significance pressure than in chickpea flours (Table 5.6). The difference in achievable deformation was also low for flours, compared to seeds. Between 124.63% – 289.29% and 84.63% – 177.66% gains in bulk density were recorded for whole seeds of chickpea and lentil while gains of 47.24% – 102.61% and 47.91% – 109.37%, respectively, were recorded for their flours, increasing from initial low gains at low magnitudes of applied pressure to appreciable gains at the higher magnitudes of axial pressure.

The side pressure factor – a product of the coefficient of wall friction and the pressure ratio – was observed to be lower for flours and higher for whole seeds (Table 5.6). The values ranged between 0.00819 – 0.0236, 0.0145 – 0.0233, 0.01360 – 0.0349 and 0.0226 – 0.0183 for chickpea flour, lentil flour, chickpea seeds and lentil seeds, respectively. Across pressures, these values were higher for lentil flour than for chickpea flour and for chickpea seeds than for lentil seeds (Table 5.6). Mean values of this parameter for chickpea flour, lentil flour, lentil seeds and chickpea seeds were 0.01335, 0.01932, 0.02190 and 0.02438, respectively. For chickpea flour, lentil flour and chickpea seed, the side pressure factor decreased progressively with increasing magnitude of applied pressure. However, for lentil seeds, this was not the case as the lateral pressure factor increased with increasing magnitude of applied pressure. This appears to be connected with the glass transition temperature of the enclosing hulls of lentil seeds which were in contact with the wall of the die and the incidence of stick during the modification of the layers in contact with the die wall as a result of the heat generated due to wall friction.

The mean kinetic coefficients of friction of the four products on mild steel surface were experimentally determined in a separate experiment and were presented in Table 5.4. These results were utilised for the computation of the pressure ratio and the lateral pressures acting on the wall of the die. The values of these parameters – pressure ratio and radial or lateral pressure for the four product forms and their variation with increasing magnitudes of applied pressure are presented in Table 5.6 and Table 5.7.

The pressure ratio was higher for seeds than it was for flours being 0.1172, 0.1159, 0.0705 and 0.04855 for chickpea seeds, lentil seeds, lentil flour and chickpea flour, respectively, in that decreasing order. Pressure ratios were higher at the lower pressures and lower at the higher pressures. The profile appears to attenuate at 450 MPa and 500 MPa.

Radial or lateral pressure exerted on the wall of the material during compression increased with increasing magnitude of applied axial pressure (Table 5.6). Average pressure on the wall of the vessel was higher for whole seeds than for flours. Mean wall pressure was higher for whole lentil seeds than for chickpea seeds (Table 5.6) and for lentil flours than for chickpea flours (Table 5.6).

Specific energy requirement during densification was also higher for whole seeds than for flours (Table 5.6). Mean energy requirement for the compression of chickpea seeds was 35.35 $kJ.kg^{-1}$. This was higher than the mean energy demand during the densification of lentil seeds, which was 27.54 $kJ.kg^{-1}$. Higher amount of energy was required for the densification of unit masses of lentil flours compared to those of chickpea flours, the values being 26.51 $kJ.kg^{-1}$ and 24.70 $kJ.kg^{-1}$, respectively. Within pressure, specific energy requirement increased, being 5.55 $kJ.kg^{-1}$ at 50 MPa and 60.08 $kJ.kg^{-1}$ at 500 MPa; elevations in energy demand per unit mass of compressed material at every 50 MPa incremental level of pressure represented significant increases in demand. Specific energy demand was 7.66 $kJ.kg^{-1}$ – 73.43 $kJ.kg^{-1}$, 5.96 $kJ.kg^{-1}$ – 57.50 $kJ.kg^{-1}$, 4.00 $kJ.kg^{-1}$ – 53.92 $kJ.kg^{-1}$ and 4.58 $kJ.kg^{-1}$ – 55.46 $kJ.kg^{-1}$ for chickpea seeds, lentil seeds, chickpea flour and lentil flours, respectively, increasing as the applied pressure increased from 50 – 500 MPa, in each case.

However, when examined in terms of specific power requirement, it was observed that more energy was expended per unit time for the compression of unit masses of food powders than was expended for the compression of unit masses of their whole seed forms (Table 5.6). Mean energy demand per unit time for the compression of flours of lentil was highest, followed by that for chickpea flour, both being 411.9 $W.kg^{-1}$ and 397.5 $W.kg^{-1}$, respectively.

More energy was also expended per unit time to compress chickpea seeds than was required for the compression of lentil seeds; the values were 397.5 $W.kg^{-1}$ and 341.7 $W.kg^{-1}$ for chickpea and lentil flours, respectively. Specific power requirements were 100.91 $W.kg^{-1}$ and 92.26 $W.kg^{-1}$ for chickpea and lentil seeds at 50 MPa and 723.63 $W.kg^{-1}$ and 658.68 $W.kg^{-1}$ for the same materials at 500 MPa. For the flours of chickpea and lentil, at 50 MPa, specific power requirements were 92.26 $W.kg^{-1}$ and 103.34 $W.kg^{-1}$; the demands were 783.31 $W.kg^{-1}$ and 777.62 $W.kg^{-1}$ for these materials, respectively, at 500 MPa.

The relative proportion of friction experienced along the interface between the compressed material and the wall of the die in comparison to the applied axial force responsible for compression was measured as the friction ratio; a graphical illustration of these measures is presented in Figure 5.1 for the lentil seeds at the mid-range pressure of 250 MPa. Compared to the applied force, it would seem that frictional resistance along the wall of the die is low, especially judging by the relative magnitudes of the two forces. Careful examination however reveals that friction represents a significant effect during compression, to the extents of having considerable influence on the transmissibility of axially applied pressure, limiting it in magnitude along the depth of the product bed, the intensity tailing off as the distance increases from the face of the piston. Additionally, thermal effects of friction does result in transformation of certain product materials, such as was experienced with the outer hulls of whole lentil seeds; where this type of effect is pronounced, a reversal of the prevalent trend in pressure ratios and the pressure ratio factor is observed, as compression progresses. In essence, as thermal effects become pronounced, the material in contact with the wall of the die transition, part of which adhere to the wall and raise performance requirements. During this study, size reduction was observed to limit this effect since, in ground products, more internal kernel materials are exposed and less covering material is exposed to the wall (Table 5.7). The ratio of friction force to the applied axial compressive force varied significantly among product forms; values of the friction force ratio were higher, on the average, for whole seeds than they were for flours and represented 4.75% and 4.29% of the total

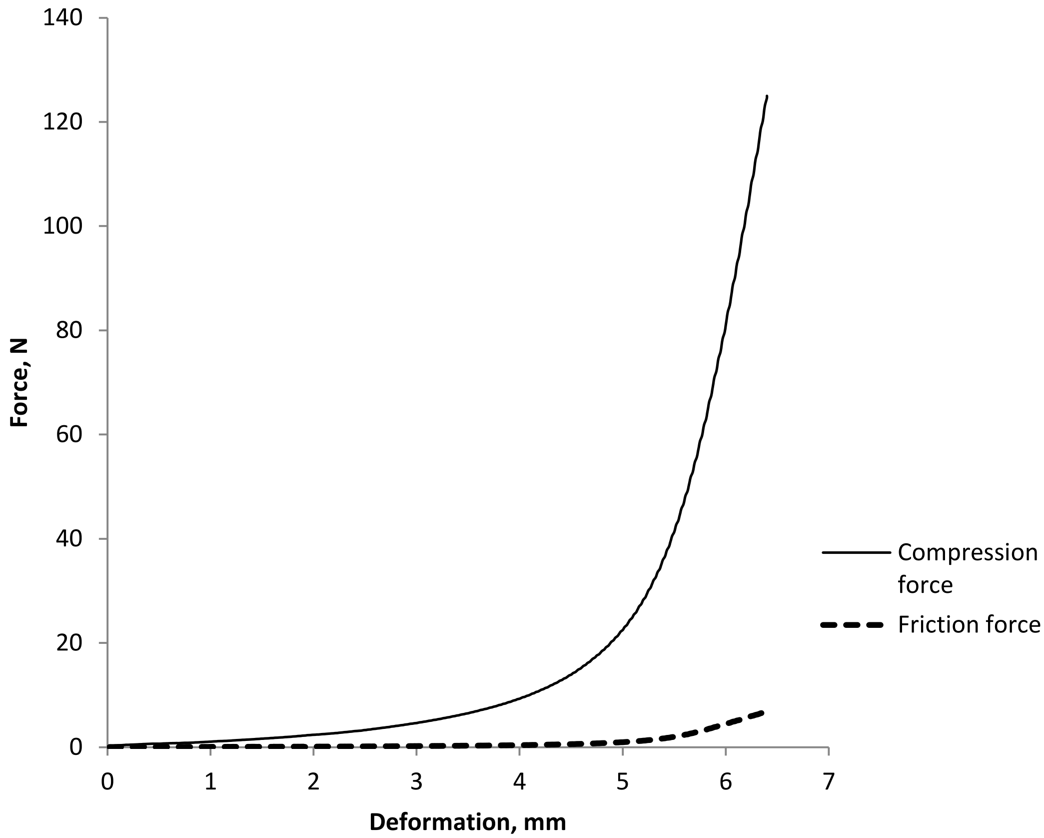

Fig. 5.1. Force deformation profile and attendant frictional resistance at 250 MPa applied pressure

applied axial compressive force, for chickpea seeds and lentil seeds or 2.63% and 3.7% of the total applied axial compressive force for chickpea and lentil flours, respectively. The ratio of friction to axial compressive force ranged between 0.01625 – 0.04610, 0.02861 – 0.04553, for chickpea flour and lentil flour and between 0.02683 – 0.06749 and 0.03595 – 0.04411 for chickpea seeds and lentil seeds, respectively, decreasing for each product form with increasing magnitude of applied pressure, except for lentil seeds for which this parameter increases with the magnitude of applied axial pressure. Size reduction and exposure of the endosperm to the wall in the case of lentil flour does reduce the effect of friction on the transformation of the hull material of the seeds of lentil; in whole seeds, as the material becomes increasingly densified and more stress is transmitted radially, the effects of heat as a result of friction on the seed coat become pronounced.

5.3. Effects of the Time Rate of Deformation and Aspect Ratio on Mechanical Behaviour of *Ceratonia siliqua* L.

The main effects of pressure, deformation rate and aspect ratio on all mechanical response parameters were highly significant (P<0.001), except for the effect of the levels of pressure considered on the rate of strain (P=0.493) and those of the time rate of deformation on specific energy (P=0.08). Significant effects were also observed at the first levels of interaction of the factors studied (Table 5.8). For instance, except for the effects on deformation and strain, which were not significant (P=0.387 and P=0.194, respectively) the interaction of the time rate of deformation and aspect ratio had highly significant effects (P<0.0029) on all mechanical response parameters. Except for the rate of strain, no significant effects on response parameters were attributable to the second level of interaction of the parameters studied.

Figure 5.2 shows the force–deformation details of compressed powder given a maximum applied pressure of 100 MPa. The profiles are curvilineal, typical of biomaterials [3, 91]. Packing improved with incremental application of compressive load [92]. Higher amount of deformation was occasioned by an increase in pressure from 50 – 100 MPa (Table 5.9). The higher the pressure, the higher will be the deformation that may be achieved. Higher rates of deformation resulted in increased deformation. These effects were, however, similar at deformation rates of 10 $mm.min^{-1}$ and 14.5 $mm.min^{-1}$ (Table 5.10). As the aspect ratio increased, deformation also increased (Table 5.11) and was significantly higher with every increase in the aspect ratio.

Table 5.8. Effects of pressure, deformation rate and aspect ratio on response variables

Response parameters	Source of variation						
	p	r_d	r_a	$p \times r_d$	$p \times r_a$	$r_d \times r_a$	$p \times r_d \times r_a$
Deformation, δ	0.001**	0.001**	0.001**	0.011*	0.001**	0.387^{ns}	0.028*
Strain, ϵ	0.001**	0.001**	0.001**	0.066^{ns}	0.001**	0.194^{ns}	0.158^{ns}
Strain rate, $\dot{\in}$	0.493^{ns}	0.001**	0.001**	0.901^{ns}	0.658^{ns}	0.001**	0.884^{ns}
Sp. energy, E_v	0.001**	0.08^{ns}	0.001**	0.003	0.001**	0.001**	0.001**
Sp. power, $\dot{E}$	0.001**	0.001**	0.001**	0.001**	0.001**	0.001**	0.349^{ns}
BDCM, ρ_C	0.001**	0.001**	0.001**	0.329^{ns}	0.317^{ns}	0.029*	0.277^{ns}
Gain, G_ρ	0.001**	0.001**	0.001**	0.329^{ns}	0.317^{ns}	0.029*	0.277^{ns}

ns = not significant at the 5% level; * = significant (at the 5% level); ** = highly significant (at the 1% level).

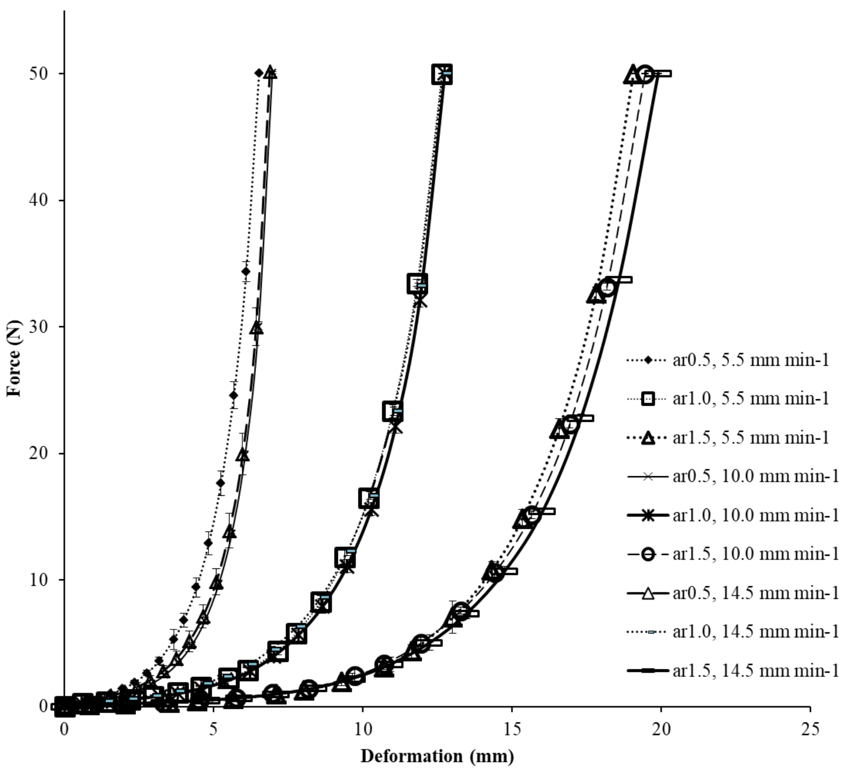

Fig. 5.2. Force – deformation profiles of carob powder at applied pressure of 100 MPa, aspect ratios (ar) of 0.5, 1.0 and 1.5 and deformation rates of 5.5, 10 and 14.5 $mm.min^{-1}$.

More strain was induced at higher pressure (Table 5.9) and at higher rates of deformation (Table 5.10); although similar amounts of strain were induced at 10 $mm.min^{-1}$ and 14.5 $mm.min^{-1}$. The highest amount of strain was obtained with the least aspect ratio (Table 5.11).

Table 5.9. Main effects of applied pressure on mechanical response parameters

Parameter	Applied pressure, p (MPa) 50	100
Deformation, δ *(mm)*	10.5[b]	11.4[a]
Strain, ϵ *(-)*	0.427[b]	0.465[a]
Strain rate, $\dot{\in}$ (s^{-1})	0.0045[a]	0.0081[a]
Specific energy, E_v (MJm^{-3})	4.70[b]	4.71[a]
Power, $\dot{E}$ $(kJm^{-3}s^{-1})$	49.7[b]	83.2[a]
Bulk density of compressed material, $\rho_C (kgm^{-3})$	1246.0[b]	1337.0[a]
Gain in bulk density, G_ρ *(%)*	75.1[b]	87.9[a]

Mean values are compared row-wise. Similar alphabets indicate homogeneous subsets. Significant effects are valid at the 5% level of significance

Table 5.10. Effects of the time rate of deformation on mechanical response

Response Parameters	Deformation rate, r_d $(mm.min^{-1})$		
	5.5	10.0	14.5
Deformation, δ *(mm)*	11.69[b]	12.11[a]	12.21[a]
Strain, ϵ *(-)*	0.4728[b]	0.4909[a]	0.4968[a]
Strain rate, $\dot{\in}$ (s^{-1})	0.0045[c]	0.0081[b]	0.0117[a]
Specific energy, E_v $(MJ.m^{-3})$	6.924[a]	6.794[a]	6.924[a]
Power, $\dot{E}$ $(kJ.m^{-3}.s^{-1})$	65.6[a]	108.8[b]	162.3[a]
Bulk density of compressed material, $\rho_C (kg.m^{-3})$	1361[b]	1429[a]	1416[a]
Gain in bulk density, G_ρ *(%)*	90.8[b]	100.3[a]	98.5[a]

Mean values are compared row-wise. Similar alphabets indicate homogeneous subsets. Significant effects are valid at the 5% level of significance

Table 5.11. Effects of aspect ratio on mechanical response

Response Parameters	Aspect ratio, r_a (-)		
	0.5	1.0	1.5
Deformation, δ *(mm)*	6.46[c]	11.67[b]	17.88[a]
Strain, ϵ *(-)*	0.5170[a]	0.4667[c]	0.4767[b]
Strain rate, $\dot{\in}$ *(s^{-1})*	0.0132[a]	0.0066[b]	0.0044[c]
Specific energy, E_v *($MJ.m^{-3}$)*	7.35[a]	6.85[b]	6.44[c]
Power, $\dot{E}$ *($kJ.m^{-3}.s^{-1}$)*	183.3[a]	95.2[b]	58.4[c]
Bulk density of compressed material, ρ_C*($kg.m^{-3}$)*	1534[a]	1374[b]	1299[c]
Gain in bulk density, G_ρ *(%)*	115.0[a]	92.6[b]	82.1[c]

Mean values are compared row-wise. Similar alphabets indicate homogeneous subsets. Significant effects are valid at the 5% level of significance

Volumetric strain – estimated as axial strain in constrained configurations – may be expressed in direct proportion to increments of pressure [92]. Void capacity is lost progressively, and is strain dependent; there is evidence that this effect is pulsatile and accounts for two notable phases during compaction [93].

Non-recoverable strain is a consistent component of induced strain [5]. Higher rates of strain were occasioned at higher deformation rates and lower aspect ratios (Tables 10 and 11). This relationship is shown in Figure 5.3. The rate of deformation is an important determinant of the rate of strain. High rates of strain have been associated with stiffer compacts [94]. The strain rate, $\dot{\in}$ (s^{-1}) may be expressed as a power function of the equipment's aspect ratio, r_a (-), at every level of deformation (Table 5.12).

$$\dot{\in} = k r_a^n \qquad (5.1)$$

where, k is proportionality constant, s^{-1} and n is exponential constant, -.

Increasing the applied pressure raises energy expenditure (Table 5.9), as does lowering the aspect ratio (Table 5.11). Energy demand decreased per unit volume of material compressed as aspect ratio became larger. The time rate of expenditure of energy increased as

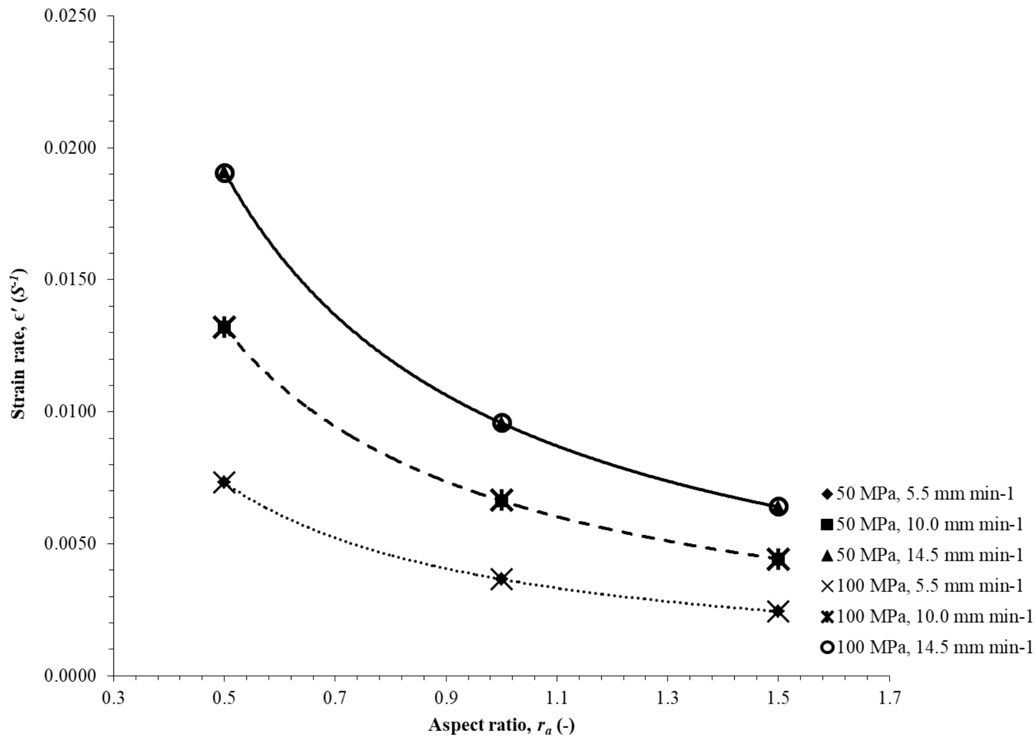

Fig. 5.3. Rates of strain in materials charged at different aspect ratios and compacted at different rates.

Table 5.12. Estimated parameters of strain rate and specific power as functions of the aspect ratio

Pressure (MPa)	Deformation rate ($mm.min^{-1}$)	Strain rate, $\dot{\in}$ (s^{-1})			Specific power, $\dot{E}$ ($J.m^{-3}.s^{-1}$)		
		k (s^{-1})	n (-)	R^2	k (s^{-1})	n (-)	R^2
50	5.5	0.0037	-0.9990	1.0000	38.7910	-1.0680	0.9928
	10.0	0.0066	-0.9930	1.0000	66.3140	-1.0880	0.9968
	14.5	0.0096	-0.9960	1.0000	96.5020	-1.1380	0.9967
100	5.5	0.0037	-0.9980	1.0000	64.8650	-1.1430	0.9990
	10.0	0.0066	-0.9930	1.0000	112.1500	-0.9400	0.9970
	14.5	0.0096	-0.9900	1.0000	167.8900	-0.9460	0.9906

deformation rate increased (Table 5.10) and as the aspect ratio was lowered. Specific power requirement is therefore lower at lower rates of deformation and higher aspect ratios, indicating patterns for energy efficiency during powder compaction. There are indications [95] that rate dependent compression response is non-linear. Considerable amount of the energy required for compaction is absorbed as plastic deformation [96], translocation of product particles being the dominant initial activity. Fluid pressure builds up within the matrix and is lost, repeatedly over the span of strain. Two positions are reported on fluid pressure build up and loss during uniaxial compression of food materials namely, repeated [93] and progressive [97]. A fourth element of energy is responsible for relaxation in the matrix after compaction. Specific power requirement was observed to be a power function of the aspect ratio (Eq. 5.2), at all rates of deformation (Figure 5.4)

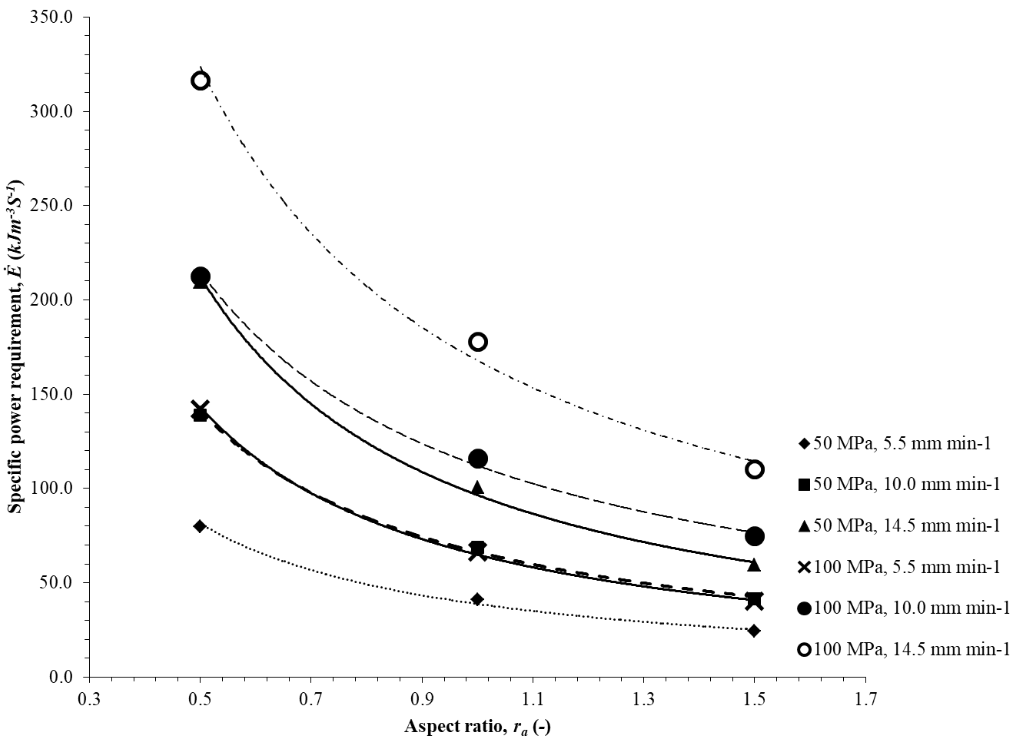

Figure 5.4. Specific power requirement at different aspect ratios and rates of deformation.

$$\dot{E} = kr_a^n \tag{5.2}$$

where, $\dot{E}$ is time rate of expenditure of energy, $J.m^{-3}.s^{-1}$, r_a is aspect ratio, -, k is constant of proportionality, s^{-1} and n is exponential constant, -. Parameters of this equation are presented in Table 4, for the different rates of deformation considered. The power law has been used to describe similar relationships such as that between the ratio of in-die to relaxed material density and aspect ratio [31].

The degree of compaction of carob powder was similar at deformation rates of 14.5 $mm.min^{-1}$ and 10.0 $mm.min^{-1}$ but higher than bulk density achieved at 5.5 $mm.min^{-1}$. Applied pressure and aspect ratio were better determinants of gain in bulk density than the time rate of deformation. Bulk density was significantly higher in material compressed at 100 MPa than those compressed at 50 MPa and represented 88% gain at applied pressure of 100 MPa over initial values, compared to gains of 75% at 50 MPa.

Given associated bulk moduli [30], applied pressure considerably determines achievable deformation, with positive correlation to energy requirement for resulting compacts [55]. Powder compacted at the least aspect ratio (Table 5.11) had the highest value of bulk density, which was 1534 $kg.m^{-3}$. Gains in bulk density increased significantly as aspect ratio was lowered.

5.4. Pressure – Density Relations of the Compression of *Lens culinaris Medik. and Cicer arietinum L.* at High Pressures

When compression data for whole seed and powder forms of chickpea and lentils in the investigated pressure regimes were fitted to exponential functional forms and relationships sought for the estimation of pressure as in terms of mean compressed material density (Figures 5.5, 5.6, 5.7 and 5.8), relationships of the form indicated in Eq. 5.1 were established (Tables 5.13, 5.15, 5.17 and 5.19). Results of the analyses of variance on these nonlinear models show that their effects at estimating pressure with respect to the density of the compressed material were highly significant ($p<0.000$). Furthermore, the coefficients of determination were significantly high; more than 99% of the response of the system was explained by each functional form presented in Tables 5.13, 5.15, 5.17 and 5.19. When the estimated model parameters were examined, each was observed to be relevant in estimating the behaviour of the system; this was true for all the product forms investigated (Tables 5.13, 5.15, 5.17 and 5.19). Model estimated effects were also found to compare favourably and to correlate positively with observed values (Tables 5.14, 5.16, 5.18 and 5.20). Further still, it could be seen that the standard errors of estimated model parameters were low. The fitted models were therefore accepted. The model has the form of the modified Gompertz function.

$$\bar{p} = a_i e^{-e^{b_i - c_i \bar{\rho}}} \quad 5.1$$

where, $\bar{p}$ is mean pressure (MPa) and $\bar{\rho}$ is mean product density (kg/m^3); a_i is a constant of proportionality (MPa) while b_i and c_i are exponential parameters and *i* is a number in reference to the product in question, namely 1, 2, 3 and 4 for chickpea seeds, chickpea flour, lentil seeds and lentil flour, respectively. The parameters of these models are summarised in Table 5.21 together with compressed material density and pressure at the point of inflection of each curve, obtained by equating the second derivative of each curve to zero. The characteristic values of pressures and density obtained at these points were between 255 MPa – 336 MPa and 1564.05 kg.m^{-3} – 1986.95 kg.m^{-3}, respectively. For each product, these densities were higher than the measured true density (Table 5.1).

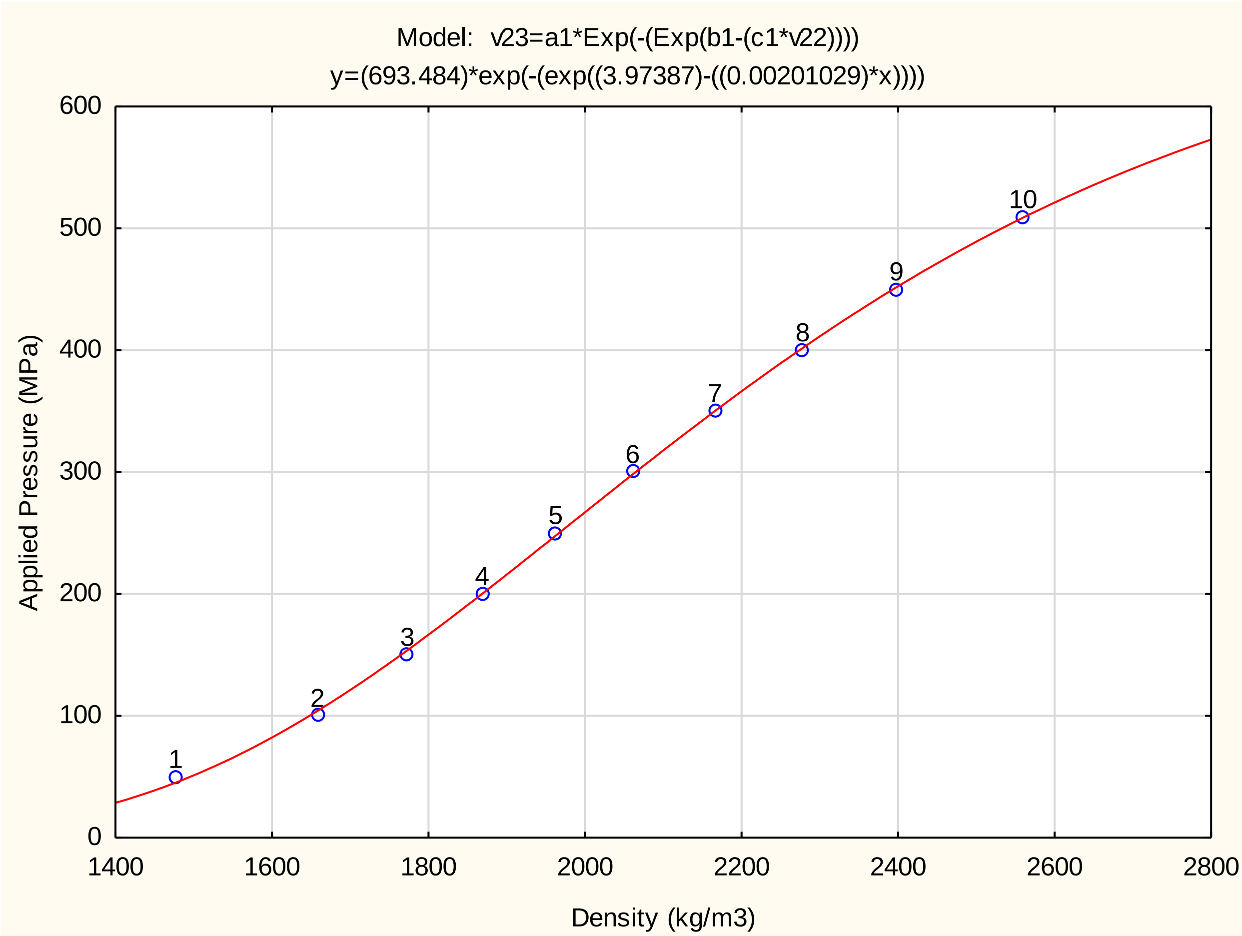

Fig. 5.5. Fitted model for the pressure density relations in bulk-compressed seeds of chickpea

Table 5.13. Estimates of model parameters for chickpea seeds

Model parameter	Estimate	Standard	t-value	P-value	Lower Confidence Limit	Upper Confidence Limit
a1 (MPa)	693.4841	15.15891	45.74762	0.000000	657.6390	729.3293
b1 (-)	3.9739	0.09293	42.76286	0.000000	3.7541	4.1936
c1 (-)	0.0020	0.00006	34.23907	0.000000	0.0019	0.0021

Table 5.14. Observed and predicted pressures for chickpea seeds

sn	Observed	Predicted	Residuals
1	50.0437	45.1007	4.94305
2	100.1605	103.8839	-3.72341
3	150.2508	153.6275	-3.37671
4	200.2246	199.9306	0.29398
5	250.1396	247.5841	2.55547
6	300.2418	297.9341	2.30765
7	350.2037	349.9442	0.25952
8	400.1598	401.7207	-1.56082
9	450.247	451.5258	-1.27876
10	509.5036	508.6834	0.82017

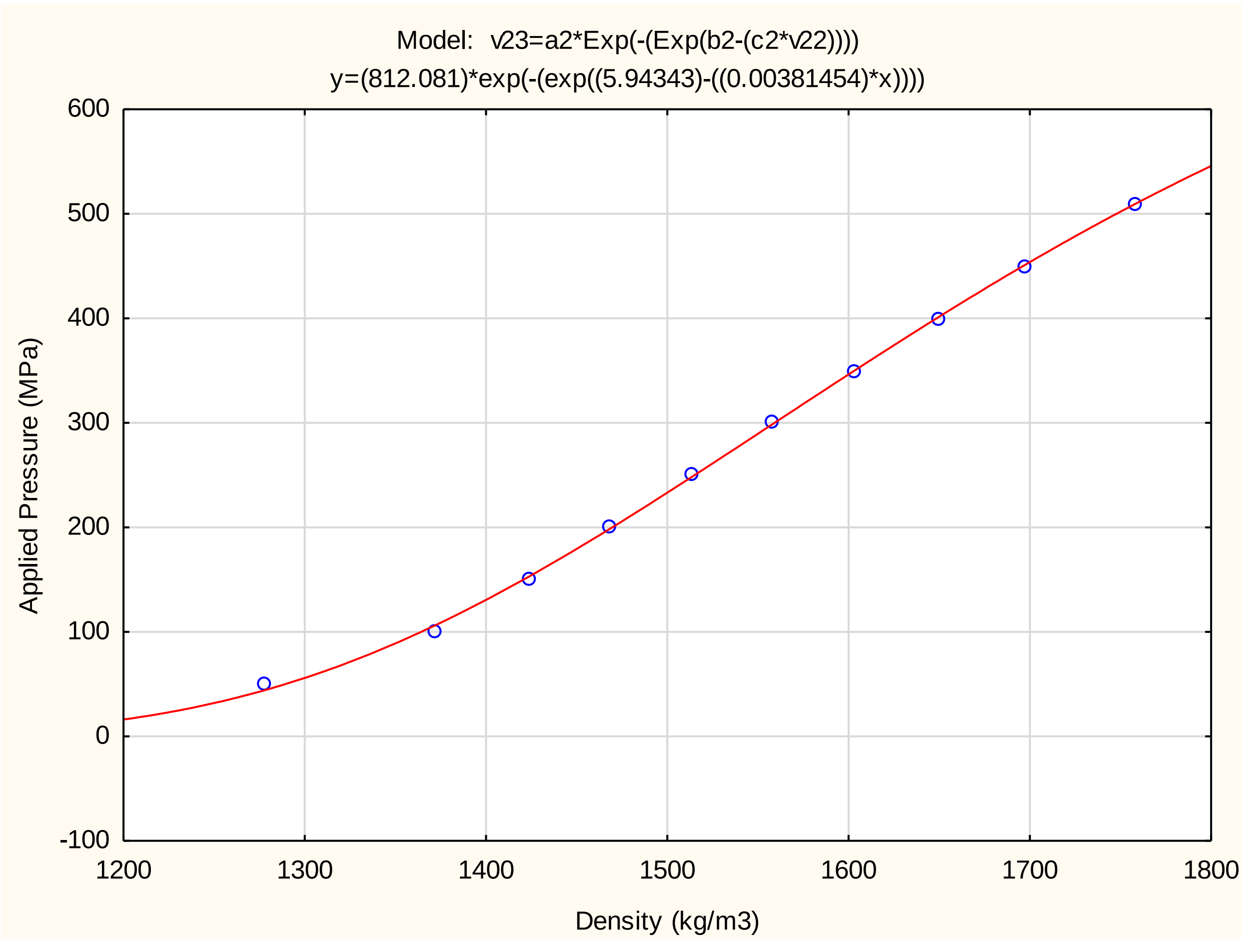

Fig. 5.6. Fitted model for pressure-density relation in compressed chickpea flour

Table 5.15. Estimate of model parameters for chickpea flour

Model parameter	Estimate	Standard	t-value	p-value	Lower Confidence Limit	Upper Confidence Limit
a2 (MPa)	812.0806	29.96649	27.09963	0.000000	741.2212	882.9401
b2 (-)	5.9434	0.19635	30.26891	0.000000	5.4791	6.4077
c2 (-)	0.0038	0.00015	25.23083	0.000000	0.0035	0.0042

Table 5.16. Observed and predicted pressures for chickpea flour

sn	Observed	Predicted	Residuals
1	50.0278	43.9883	6.03957
2	100.1606	106.0084	-5.84788
3	150.2729	152.6512	-2.37825
4	200.2454	198.7347	1.51074
5	250.221	248.3651	1.8559
6	300.2342	298.5968	1.63741
7	350.2006	350.0518	0.14873
8	400.3771	401.3595	-0.98239
9	450.2097	450.9475	-0.73776
10	509.558	509.279	0.27905

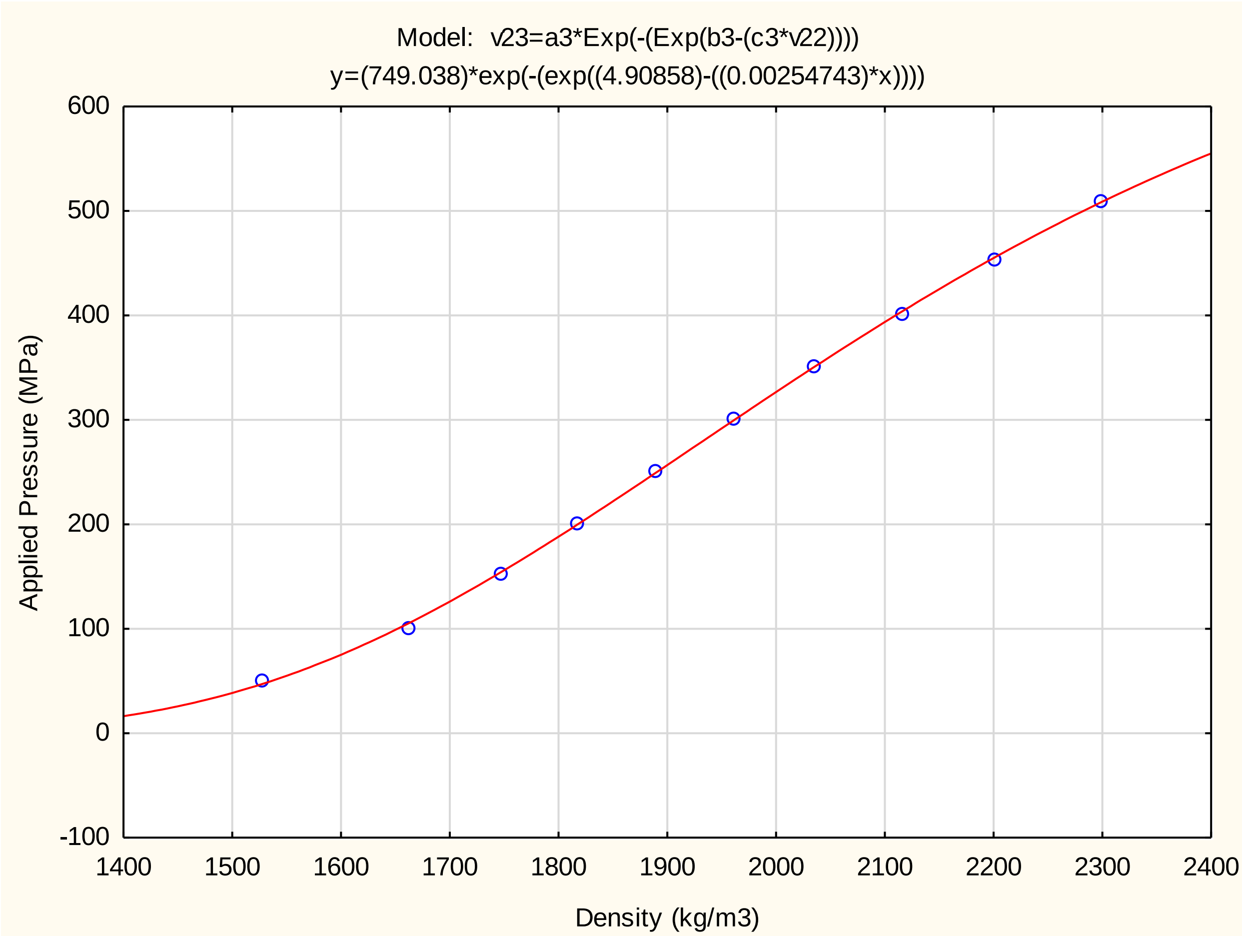

Fig. 5.7. Fitted model for the pressure density relations in bulk-compressed lentil seeds

Table 5.17. Estimate of model parameters for lentil seeds

Model parameter	Estimate	Standard	t-value	P-value	Lower Confidence Limit	Upper Confidence Limit
a3	749.0382	16.33931	45.84271	0.000000	710.4018	787.6745
b3	4.9086	0.10442	47.00592	0.000000	4.6617	5.1555
c3	0.0025	0.00007	38.42440	0.000000	0.0024	0.0027

Table 5.18. Observed and predicted pressures for lentil seeds

sn	Observed	Predicted	Residuals
1	50.459	47.3526	3.10642
2	101.3502	104.935	-3.58482
3	151.763	153.479	-1.71596
4	200.6456	199.939	0.70658
5	251.9626	249.62	2.34255
6	300.7989	299.038	1.76097
7	350.6301	350.6547	-0.02456
8	401.9359	403.8381	-1.90222
9	453.3028	455.0452	-1.7424
10	509.6296	508.0362	1.59338

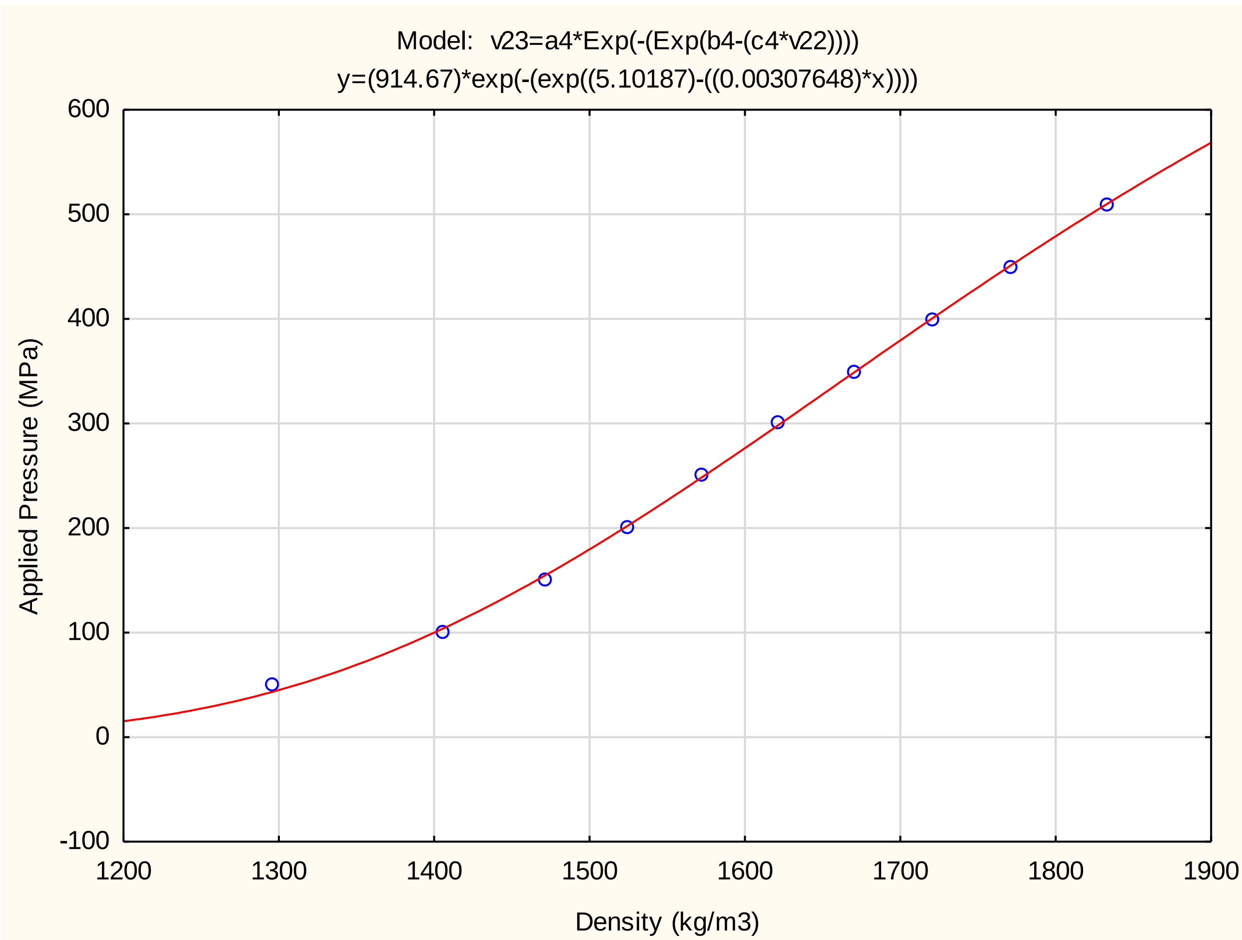

Fig. 5.8. Fitted model for pressure-density relation in compressed lentil flour

Table 5.19. Estimated model parameters for lentil flour

Model parameter	Estimate	Standard	t-value	P-value	Lower Confidence Limit	Upper Confidence Limit
a4	914.6701	45.45143	20.12412	0.000000	807.1945	1022.146
b4	5.1019	0.18699	27.28384	0.000000	4.6597	5.544
c4	0.0031	0.00014	21.37238	0.000000	0.0027	0.003

Table 5.20. Observed and predicted pressures for lentil flour

sn	Observed	Predicted	Residuals
1	50.0608	43.0439	7.01686
2	100.1304	103.3970	-3.26662
3	150.2461	154.9622	-4.71614
4	200.2105	201.5027	-1.29225
5	250.2128	248.2457	1.96718
6	300.2940	297.9466	2.34733
7	350.2260	348.2713	1.95476
8	400.1907	400.6587	-0.46797
9	450.2219	450.8957	-0.67373
10	509.5655	510.2520	-0.68651

Table 5.21. Summary of model parameters

Product	a	b	c	R^2	P-value	$\bar{\rho}_s$	$\bar{p}_s$
Chickpea seed	693.4840	3.9739	0.0020	0.9990	0.000	1986.95	255.119
Chickpea flour	812.0810	5.9434	0.0038	0.9999	0.000	1564.05	298.745
Lentil seed	749.0382	4.9086	0.0025	0.9999	0.000	1963.44	275.556
Lentil flour	914.6700	5.1019	0.0031	0.9998	0.000	1645.77	336.484

6. Summary, Conclusions and Recommendations

6.1. Summary

The behaviour of three agricultural materials in different forms was studied with a view to understanding their mechanical responses under high hydrostatic pressure. The effects of selected crop, machine and process parameters were considered, namely those of product type and form and magnitude of applied pressure; the effects also of the time rate of deformation and the equipment aspect ratios were considered. Physical properties of the test materials relevant to their densification were determined and employed for the computation of relevant compression parameters while providing understanding on the nature and flowability of some of the materials studied. Compression tests were implemented using factorial experiments fitted into completely randomised designs for evaluation of the effects of the treatment parameters. Test data were subjected to the analysis of variance and treatment means were compared using Duncan's multiple range test. Functional forms were fitted to some observed response trends using nonlinear estimation and validation procedures. All the factors considered had significant effects on the behaviour of the agricultural products. Estimate statistics for the various functional forms indicate that they model the responses sought satisfactorily.

6.2. Conclusions

Product form and applied pressure have highly significant effects on mechanical response of the selected agricultural materials. Strain increased as the magnitude of applied pressure increased and was higher in whole seeds than in flours. The level of strain differed with each crop. The rate of strain had no dependence on the magnitude of applied pressure and was similar for all but one of the product forms. Bulk density of compressed materials had positive dependence on applied pressure, as well as the gain in bulk density; bulk density gain was higher for whole seed forms than for flours. The radial pressure acting on the wall of the compression vessel increased as did the magnitude of applied pressure and was greatest at the highest pressure, being higher for whole seeds than it was for flours. Side pressure was found to vary with the compressed material or crop. The magnitude of applied pressure influenced compression energy demand significantly; these two parameters correlated positively, as did also the time rate of expenditure of energy with applied pressure. Whereas energy demand per unit mass of compressed material was higher for whole seeds than for flours, the time rate of expenditure of energy, per unit mass of compressed material – or specific power requirement – was greater in flours than it was in whole seeds. For every mass of material compressed, therefore, more energy is expended per unit time in flours than in whole seeds.

Applied pressure, time rate of deformation and aspect ratio and their interactions had pronounced effects on the behaviour of the carob powder. By increasing applied pressure, elevations in energy demand are incurred. Reducing the rate at which the materials are deformed also increased energy demand for deformation. Energy demand was found to decrease as aspect ratios became larger. Whereas better product densification was achieved at the lower aspect ratios, this study showed that energy efficiency improves quite significantly when aspect ratios are enlarged. Both specific power and the rate of strain may be satisfactorily described as power functions of the aspect ratio.

The dependence of mean applied pressure on the average density of the compressed material may be described using the modified Gompertz function – an exponential form. This function satisfactorily described the trends in the studied pressure range and did not require separate modelling of different regions of observed responses using alternative functional forms as were done in existing studies. The function fits were found to be satisfactory, judging by the parameter estimates and the reported statistics.

Energy requirement in equipment employed for the densification of the food materials tested may be estimated as exponential functions of the desired product densities, as described, for the range of pressures reported. Comminuted forms of each crop material require less energy to work and the effects of friction on flours is less pronounced. Pressure exerted laterally on the walls of the vessel is also lower with flours than with whole grains. During the production of densified food cakes or their expanded alternatives in high pressure, short duration high temperature schemes, therefore, modifying the materials into flours may prove more profitable and impart less wear on such presses. Results from this study are also of importance during the handling and storage of these materials, especially with regard to the flow of food powders, agglomeration and efficient storage.

6.3. Recommendations

The applicability of the established functional form to other agricultural products of the nature investigated in this study are recommended for the purpose of verification; estimates of model parameters are likely to vary for different crops and their forms but may be established using less cumbersome experiments. The influence of moisture on the functional form may also be investigated. One immediate application of the findings in this study is with respect to the manufacture of ready to eat snacks and cereals, especially by employing very high pressure and short duration, high temperature product modification procedures. Studies in this area are scantily reported.

7. References

[1] FABORODE, M. O. a J. R. O'CALLAGHAN. Theoretical analysis of the compression of fibrous agricultural materials. *Journal of Agricultural Engineering Research* [online]. 1986, **35**(3), 175–191. ISSN 00218634. Dostupné z: doi:10.1016/S0021-8634(86)80055-5

[2] BLAHOVEC, Jiří. Fenomenologický model průběhu stlačo- vání stébelnatých materiálů [Phenomenological model of compression processing of stalk materials]. *Zemědělská Technika*. 1984, **9**, 545–555.

[3] BLAHOVEC, Jiří. Stlačování upravené žitné slámy [Compaction of modified rye straw]. *Zemědělská Technika*. 1982, **28**(2), 65–75.

[4] NONA, Kenny D., Bart LENAERTS, Erdal KAYACAN a Wouter SAEYS. Bulk compression characteristics of straw and hay. *Biosystems Engineering* [online]. 2014, **118**(1), 194–202. ISSN 15375110. Dostupné z: doi:10.1016/j.biosystemseng.2013.12.005

[5] O'DOGHERTY, M. J. A review of the mechanical behaviour of straw when compressed to high densities. *Journal of Agricultural Engineering Research* [online]. 1989, **44**, 241–265. ISSN 00218634. Dostupné z: doi:10.1016/S0021-8634(89)80086-1

[6] BLAHOVEC, Jiří, K. PATOČKA a B. SZOT. Stlačování suché slámy základních obilnin při nižších tlacích [compression of dry straw of common cereals at low pressures]. *Zemědělská Technika*. 1985, **31**(3), 129–142.

[7] BLAHOVEC, Jiří a O. KUBÁT. Stlačovaní suchých zemědělských porézních materialů [Compression of dry porous agricultural materials at high pressures]. *Zemědělská Technika*. 1987, **33**(5), 289–302.

[8] MIAO, Z., T.E. GRIFT a K.C. TING. *Size reduction and densification of lignocellulosic biomass feedstock for biopower , bioproducts , and liquid biofuel production* [online]. 2014. Dostupné z: doi:10.1081/E-EAFE2-120051298

[9] JAFARI, Morteza, Arash KOOCHEKI a Elnaz MILANI. Effect of extrusion cooking on

chemical structure, morphology, crystallinity and thermal properties of sorghum flour extrudates. *Journal of Cereal Science* [online]. 2017, **75**, 324–331. ISSN 10959963. Dostupné z: doi:10.1016/j.jcs.2017.05.005

[10] SAYANJALI, Sara, Danyang YING, Luz SANGUANSRI, Roman BUCKOW, Mary Ann AUGUSTIN a Sally L. GRAS. The effect of extrusion on the functional properties of oat fibre. *LWT - Food Science and Technology* [online]. 2017, **84**, 106–113. ISSN 00236438. Dostupné z: doi:10.1016/j.lwt.2017.05.025

[11] SALLEH, F. S.Mohd, Y. A. YUSOF, M. S. ANUAR a N. L. CHIN. Understanding the tabletting characteristics of Ficus deltoidea powder by fitting into compression models. *Journal of Food Process Engineering* [online]. 2015, **38**(3), 250–261. ISSN 17454530. Dostupné z: doi:10.1111/jfpe.12165

[12] DOBRZAŃSKI, B a A STĘPNIEWSKI. Physical properties of seeds in technological processes. In: Stanislaw Grundas and Andrzej STEPNIEWSKI, ed. *Advances in Agrophysical Research* [online]. B.m.: InTech, 2013, s. 269–294. ISBN 9789535111849. Dostupné z: doi:10.5772/3341

[13] CAI, Weizhao, Andrzej GŁADYSIAK, Michalina ANIOŁA, Vincent J. SMITH, Leonard J. BARBOUR a Andrzej KATRUSIAK. Giant Negative Area Compressibility Tunable in a Soft Porous Framework Material. *Journal of the American Chemical Society* [online]. 2015, **137**(29), 9296–9301. ISSN 15205126. Dostupné z: doi:10.1021/jacs.5b03280

[14] CONSIDINE, Kiera M., Alan L. KELLY, Gerald F. FITZGERALD, Colin HILL a Roy D. SLEATOR. High-pressure processing - Effects on microbial food safety and food quality. *FEMS Microbiology Letters* [online]. 2008, **281**(1), 1–9. ISSN 03781097. Dostupné z: doi:10.1111/j.1574-6968.2008.01084.x

[15] PATTERSON, Margaret F, Michele QUINN, Ryan SIMPSON a Arthur GILMOUR. Sensitivity of Vegetative Pathogens to High Hydrostatic Pressure Treatment in Phosphate-Buffered Saline and Foods. *Journal of Food Protection* [online]. 1995, **58**(5), 524–529. ISSN 0362028X. Dostupné z: doi:10.4315/0362-028X-58.5.524

[16] TUMULURU, J.S., C.T. WRIGHT, J.R. HESS a K.L. KENNEY. A review of biomass densification systems to develop uniform feedstock commodities for bioenergy application. *Biofuels, Bioproducts and Biorefining* [online]. 2011, **5**(6), 683–707. ISSN 1932104X. Dostupné z: doi:10.1002/bbb.324

[17] AREMU, A K, A A ADEMUWAGUN a C A OGUNLADE. Effects of moisture content and loading orientation on some mechanical properties of the african oil bean seed (Pentaclethra Macrophylla Benth). *African Journal of Agricultural Research* [online]. 2014, **9**(49), 3504–3510. Dostupné z: doi:10.5897/AJAR2014.9109

[18] ALTUNTAS, Ebubekir a Hilal DEMIRTOLA. Effect of moisture content on physical properties of some grain legume seeds. *New Zealand Journal of Crop and Horticultural Science* [online]. 2007, **35**(4), 423–433. ISSN 0114-0671. Dostupné z: doi:10.1080/01140670709510210

[19] HADNAĐEV, Tamara Dapčević, Aleksandra TORBICA a Miroslav HADNAĐEV. Rheological properties of wheat flour substitutes/alternative crops assessed by Mixolab. *Procedia Food Science* [online]. 2011, **1**, 328–334. ISSN 2211601X. Dostupné z: doi:10.1016/j.profoo.2011.09.051

[20] CHANVRIER, Hélène, Guy Della VALLE a Denis LOURDIN. Mechanical behaviour of corn flour and starch-zein based materials in the glassy state: A matrix-particle interpretation. *Carbohydrate Polymers* [online]. 2006, **65**(3), 346–356. ISSN 01448617. Dostupné z: doi:10.1016/j.carbpol.2006.01.027

[21] TUMULURU, Jaya Shankar, Christopher T. WRIGHT, Kevin L. KENNY a J. Richard HESS. *A Review on biomass densification technologies for energy application* [online]. Idaho Falls: Idaho National Laboratory, U.S. Department of Energy. 2010. Dostupné z: doi:10.1017/CBO9781107415324.004

[22] NONA, Kenny D., Bart LENAERTS, Erdal KAYACAN a Wouter SAEYS. Bulk compression characteristics of straw and hay. *Biosystems Engineering* [online]. 2014, **118**(1), 194–202. ISSN 15375110. Dostupné z: doi:10.1016/j.biosystemseng.2013.12.005

[23] MORROW, C. T. a N. N. MOHSENIN. Consideration of selected agricultural products as viscoelastic materials. *Journal of Food Science* [online]. 1966, **31**(5), 686–698. ISSN 17503841. Dostupné z: doi:10.1111/j.1365-2621.1966.tb01925.x

[24] FINNEY, E. E. *The Viscoelastic Behavior of the Potato, Solanum Tuberosum Under Quasi-Static Loading*. B.m., 1963. Michigan State University.

[25] MANI, S, L G TABIL a S SOKHANSANJ. Evaluation of compaction equations applied to four biomass species. *Canadian Biosystems Engineering*. 2004, **46**, 55–61. ISSN 14929058.

[26] CHAPMAN, Kent D., John M. DYER a Robert T. MULLEN. Biogenesis and functions of lipid droplets in plants. *Journal of Lipid Research* [online]. 2012, **53**(2), 215–226. ISSN 0022-2275. Dostupné z: doi:10.1194/jlr.R021436

[27] MREMA, G C a P B MCNULTY. Microstructure of rapeseed and cashew as related to mechanical oil expression. *Ir. J. Fd. Sci. Technol.* 1984, **8**, 59–66. ISSN 03070492.

[28] KANIT, Toufik, Franck N'GUYEN, Samuel FOREST, Dominique JEULIN, Matt REED a Scott SINGLETON. Apparent and effective physical properties of heterogeneous materials: Representativity of samples of two materials from food industry. *Computer Methods in Applied Mechanics and Engineering* [online]. 2006, **195**(33–36), 3960–3982. ISSN 00457825. Dostupné z: doi:10.1016/j.cma.2005.07.022

[29] JOHNSON, Praveen, Jitendra PALIWAL a Stefan CENKOWSKI. Analysing the effect of particle size on the disintegration of distiller's spent grain compacts while drying in superheated steam medium. *Biosystems Engineering* [online]. 2015, **134**, 105–116. ISSN 15375110. Dostupné z: doi:10.1016/j.biosystemseng.2015.04.005

[30] JOHNSON, Praveen, Stefan CENKOWSKI a Jitendra PALIWAL. Compaction and relaxation characteristics of single compacts produced from distiller's spent grain. *Journal of Food Engineering* [online]. 2013, **116**(2), 260–266. ISSN 02608774. Dostupné z: doi:10.1016/j.jfoodeng.2012.11.025

[31] O'DOGHERTY, M. J. a J. A. WHEELER. Compression of straw to high densities in closed cylindrical dies. *Journal of Agricultural Engineering Research* [online]. 1984, **29**(1), 61–72. ISSN 00218634. Dostupné z: doi:10.1016/0021-8634(84)90061-1

[32] RAHAMAN, Sheikh Aminur a P Abdul SALAM. Characterization of cold densified rice straw briquettes and the potential use of sawdust as binder. *Fuel Processing Technology* [online]. 2017, **158**, 9–19. ISSN 0378-3820. Dostupné z: doi:10.1016/j.fuproc.2016.12.008

[33] LAM, Pak Yiu, Pak Sui LAM, Shahab SOKHANSANJ, Xiaotao T. BI, C. Jim LIM a Staffan MELIN. Effects of pelletization conditions on breaking strength and dimensional stability of Douglas fir pellet. *Fuel* [online]. 2014, **117**(PARTB), 1085–1092. ISSN 00162361. Dostupné z: doi:10.1016/j.fuel.2013.10.033

[34] TUMULURU, Jaya Shankar. Effect of process variables on the density and durability of the pellets made from high moisture corn stover. *Biosystems Engineering* [online]. 2014, **119**, 44–57. ISSN 15375110. Dostupné z: doi:10.1016/j.biosystemseng.2013.11.012

[35] BARGALE, P.C., J.M. IRUNDAYARAJ a B. MARQUIS. Some mechanical properties and stress relaxation characteristics of lentils - part II.pdf. *Canadian agricultural engineering*. 1994, **36**(4), 251–254.

[36] BLAHOVEC, Jiří. Elastic and strength properties of round agricultural products. *International Agrophysics*. 1994, **8**, 543–546.

[37] LASKOWSKI, Janusz a Grzegorz LYSIAK. Use of compression behaviour of legume seeds in view of impact grinding prediction. *Powder Technology* [online]. 1999, **105**(1–3), 83–88. ISSN 00325910. Dostupné z: doi:10.1016/S0032-5910(99)00121-7

[38] BABIC, L. J., M. RADOJEIN, I. PAVKOV, M. BABIC, J. TURAN, M. ZORANOVIC a S. STANISIC. Physical properties and compression loading behaviour of corn seed. *International Agrophysics* [online]. 2013, **27**(2), 119–126. ISSN 02368722. Dostupné

z: doi:10.2478/v10247-012-0076-9

[39] LASKOWSKI, Janusz, Grzegorz ŁYSIAK a Stanisław SKONECKI. Material properties in grinding and agglomeration. In: Józef HORABIK a Janusz LASKOWSK, ed. *Mechanical properties of granular agro-materials and food powders for industrial practice, Part II*. Lublin: Institute of Agrophysics PAS, 2005, s. 47–86. ISBN 8389969351.

[40] MONEDERO, Esperanza, Henar PORTERO a Magín LAPUERTA. Pellet blends of poplar and pine sawdust: Effects of material composition, additive, moisture content and compression die on pellet quality. *Fuel Processing Technology* [online]. 2015, **132**, 15–23. ISSN 03783820. Dostupné z: doi:10.1016/j.fuproc.2014.12.013

[41] KARWE, M V. *Food Engineering*. B.m.: UNESCO, 2009.

[42] MIAO, Zewei, James W. PHILLIPS, Tony E. GRIFT a Sunil K. MATHANKER. Measurement of mechanical compressive properties and densification energy requirement of Miscanthus x giganteus and Switchgrass. *Bioenergy Research* [online]. 2015, **8**(1), 152–164. ISSN 19391242. Dostupné z: doi:10.1007/s12155-014-9495-8

[43] ADAPA, Phani K, Lope G TABIL a Greg J SCHOENAU. Factors affecting the quality of biomass pellet for biofuel and energy analysis of pelleting process. *Internationl Journal of Agricultural and Biological Engineering* [online]. 2013, **6**(2), 1–12. Dostupné z: doi:10.3965/j.ijabe.20130602.001

[44] MEDIAVILLA, I., L. S. ESTEBAN a M. J. FERNÁNDEZ. Optimisation of pelletisation conditions for poplar energy crop. *Fuel Processing Technology* [online]. 2012, **104**, 7–15. ISSN 03783820. Dostupné z: doi:10.1016/j.fuproc.2012.05.031

[45] LEE, Soo min, Byoung Jun AHN, Don Ha CHOI, Gyu-Seong HAN, Han-Seob JEONG, Sye Hee AHN a In YANG. Effects of densification variables on the durability of wood pellets fabricated with Larix kaempferi C. and Liriodendron tulipifera L. sawdust. *Biomass and Bioenergy* [online]. 2013, **48**, 1–9. ISSN 09601481. Dostupné z: doi:10.1016/j.renene.2013.06.038

[46] BLAHOVEC, Jiří. Role of water content in food and product texture. *International Agrophysics*. 2007, **21**, 209–215.

[47] PUIG-ARNAVAT, Maria, Lei SHANG, Zsuzsa SÁROSSY, Jesper AHRENFELDT a Ulrik B. HENRIKSEN. From a single pellet press to a bench scale pellet mill - Pelletizing six different biomass feedstocks. *Fuel Processing Technology* [online]. 2016, **142**, 27–33. ISSN 03783820. Dostupné z: doi:10.1016/j.fuproc.2015.09.022

[48] KALIYAN, Nalladurai a R. Vance MOREY. Constitutive model for densification of corn stover and switchgrass. *Biosystems Engineering* [online]. 2009, **104**(1), 47–63. ISSN 15375110. Dostupné z: doi:10.1016/j.biosystemseng.2009.05.006

[49] FABORODE, M. O. Moisture effects in the compaction of fibrous agricultural residues. *Biological Wastes* [online]. 1989, **28**(1), 61–71. ISSN 02697483. Dostupné z: doi:10.1016/0269-7483(89)90050-5

[50] HARUN, Noorfidza Y. a Muhammad T. AFZAL. Effect of particle size on mechanical properties of pellets made from biomass blends. *Procedia Engineering* [online]. 2016, **148**, 93–99. ISSN 18777058. Dostupné z: doi:10.1016/j.proeng.2016.06.445

[51] WEIDINGER, P., W. BLUM, U. HUNSCHE a A. HAMPEL. The influence of friction on plastic deformation in compression tests. *Physica Status Solidi (a)*. 1996, **156**, 305–315.

[52] MENG, X., D. THREINEN, M. HANSEN a D. DRIEDGER. Effects of extrusion conditions on system parameters and physical properties of a chickpea flour-based snack. *Food Research International* [online]. 2010, **43**(2), 650–658. ISSN 09639969. Dostupné z: doi:10.1016/j.foodres.2009.07.016

[53] BRENT, J L, S J MULVANEY, C COHEN a J a BARTSCH. Thermomechanical glass transition of extruded cereal melts. *Journal of Cereal Science* [online]. 1997, **26**, 301–312. ISSN 07335210. Dostupné z: doi:doi:10.1006/jcrs.1997.0140

[54] MANI, S., L. G. TABIL a S. SOKHANSANJ. Evaluation of compaction equations applied to four biomass species. *Canadian Biosystems Engineering*. 2004, **46**, 55–61.

ISSN 14929058.

[55] ADAPA, Phani, Lope TABIL a Greg SCHOENAU. A Comprehensive analysis of the factors affecting densification of barley, canola, oat and wheat straw grinds. In: *CSBE/SCGAB 2011 Annual Conference*. 2013, s. Paper No. CSBE11-513.

[56] SKALWEIT, H. Kräfte und Beanspruchungen in Strohpressen (Forces and stresses in straw presses). *4 Konstrukteur-Kursus. RKTL*. 1938, **88**, 1–8.

[57] MEWES, E. Zum Verhalten yon Pressgutern in Prestopfen (On the behaviour of compressed matter in pressure chambers). *Landtechnische Forshung*. 1958, **8**(6), 158–164.

[58] OSOBOV, V. I. Theoretical principles of compressing fibrous plant materials. *Trudy Viskhom*. 1967, **55**, 221–265.

[59] UZIAK, J. Usefulness of different representations of the material in the pressing chamber of a baler to dynamic analysis of a pressing system. In: Vincent A. DODD a Patrick M. GRACE, ed. *Proceedings of the 11th International Congress on Agricultural Engineering*. 1989, s. 2031–2035.

[60] MATTHIES, H. J. a W. BUSSE. Neuere Erkeuntnisse auf dem Gebiete des Verdichtens von Halmgntnut hohem Normaldruck (New information on the compaction of fodder materials with high loads). *Grundlagen der Landtechnik*. 1966, **16**(3), 87–92.

[61] CHENG, Xuduo, Qiang ZHANG, Xiaojie YAN a Cuixia SHI. Compressibility and equivalent bulk modulus of shelled corn. *Biosystems Engineering* [online]. 2015, **140**(2013), 91–97. ISSN 15375110. Dostupné z: doi:10.1016/j.biosystemseng.2015.10.001

[62] SITKEI, Gyorgy. *Mechanics of agricultural materials*. Amsterdam: Elsevier, 1986.

[63] KONATE, Ibrahim, Abdelkarim FILALI-MALTOUF a El Bekkay BERRAHO. Diversity analysis of moroccan carob (Ceratonia siliqua L.) accessions using phenotypic traits and RAPD markers. *Acta Botanica Malacitana*. 2007, **32**, 79–90.

[64] SÁNCHEZ, S., L. J. LOZANO, C. GODÍNEZ, D. JUAN, A. PÉREZ a F. J. HERNÁNDEZ. Carob

pod as a feedstock for the production of bioethanol in Mediterranean areas. *Applied Energy* [online]. 2010, **87**(11), 3417–3424. ISSN 03062619. Dostupné z: doi:10.1016/j.apenergy.2010.06.004

[65] YOUSIF, Ali K. a H.M. ALGHZAWI. Processing and characterization of carob powder. *Food Chemistry*. 2000, **69**, 283–287.

[66] CRAIG, WINSTON J. a THUY T. NGUYEN. Caffeine and Theobromine levels in cocoa and carob products. *Journal of Food Science* [online]. 1984, **49**(1), 302–303. ISSN 17503841. Dostupné z: doi:10.1111/j.1365-2621.1984.tb13737.x

[67] FAO. *FAOSTAT Database* [online]. Rome, Italy: FAO, 2018. Dostupné z: http://www.fao.org/faostat/en/#data/QC/visualize

[68] JOSHI, Matina, Yakindra TIMILSENA a Benu ADHIKARI. Global production, processing and utilization of lentil: A review. *Journal of Integrative Agriculture* [online]. 2017, **16**(12), 2898–2913. ISSN 20953119. Dostupné z: doi:10.1016/S2095-3119(17)61793-3

[69] UEBERSAX, M.A. a D.G. OCCENA. *Legumes in the diet*. 2nd vyd. B.m.: Academic Press, London, 2003.

[70] GRANT, G., M. DUNCAN, R. ALONSO a F. MARZO. *Peas and Lentils*. 2nd vyd. B.m.: Academic Press, London, 2003.

[71] LAM, Y. a B.O. DE LUMEN. *Legumes: Dietary importance*. B.m.: Academic Press, London, 2003.

[72] QUINN, Gerry P. a Michael J. KEOUGH. *Experimental design and data analysis for biologists*. Cambridge: Cambridge University Press, 2002. ISBN 9780521811286.

[73] KUTNER, Michael H., Christopher J. NACHTSHEIM, John NETER a William LI. *Applied Linear Statistical Models*. 5. vyd. Chicago: McGraw-Hill, 2005.

[74] ASABE. *S352.2: Moisture measurement -unground grain and seeds*. 1988.

[75] INTERNATIONAL ORGANIZATION FOR STANDARDIZATION. *ISO 712: 2009, Cereals and*

cereal products -- Determination of moisture content -- Reference method. 2009

[76] CHANG, C.S. Measuring density and porosity of grain kernels using a gas pycnometer. *Cereal Chemistry*. 1988, **65**(1), 13–15.

[77] SEMEL, F. J. a D. A. LADOS. Porosity analysis of PM materials by helium pycnometry. *Powder Metallurgy* [online]. 2006, **49**(2), 173–182. ISSN 0032-5899. Dostupné z: doi:10.1179/174329006X95347

[78] ASTM INTERNATIONAL. ASTM D7481-18, Standard test methods for determining loose and tapped bulk densities of powders using a graduated cylinder. *Annual Book of ASTM Standards* [online]. 2018. Dostupné z: doi:10.1520/D7481-09.1

[79] WORLD HEALTH ORGANIZATION. *Bulk density and tapped density of powders*. 2018.

[80] UNITED STATES PHARMACOPEIAL CONVENTION, USPC. *Bulk density and tapped density of powders* [online]. 2014. Dostupné z: https://www.usp.org/sites/default/files/usp/document/harmonization/gen-chapter/bulk_density.pdf

[81] SIRISOMBOON, P., P. KITCHAIYA, T. PHOLPHO a W. MAHUTTANYAVANITCH. Physical and mechanical properties of Jatropha curcas L. fruits, nuts and kernels. *Biosystems Engineering*. 2007, **97**, 201–207. ISSN 15375110.

[82] MOHSENIN, N.N. *Physical properties of plant and animal materials. Vol. I: Structure, physical characteristics and mechanical properties*. New York: Gordon and Breach Science Publishers, 1986.

[83] BLAHOVEC, Jiří. Fenomenologický model průběhu stlačo- vání stébelnatých materiálů [Phenomenological model of the compression of stalky materials]. *Zemědělská Technika*. 1984, **30**(9), 545–555.

[84] EVON, Ph, I. AMALIA KARTIKA, M. CERNY a L. RIGAL. Extraction of oil from jatropha seeds using a twin-screw extruder: Feasibility study. *Industrial Crops and Products*. 2013, **47**, 33–42. ISSN 09266690.

[85] CHAPRA, S.C. a R.P. CANALE. *Numerical methods for engineers*. 7th vyd. New York: McGraw-Hill Education, 2015.

[86] DRAPER, N. R. a H. SMITH. *Applied Regression Analysis*. 3rd vyd. New York: John wiley & Sons, Inc., 1998.

[87] MOHSENIN, N.N. *Physical properties of plant and animal materials. Vol I: structure, physical characteristics and mechanical properties*. 2nd vyd. New York: Gordon and Breach Science Publishers, 1986.

[88] UNITED STATES PHARMACOPEIAL CONVENTION, USPC. *Powder flow* [online]. 2016. Dostupné z: http://www.usp.org/sites/default/files/Harmonization/Gen-Chapter/g05_pf_30_6_2004.pdf

[89] CARMAN, K. Some physical properties of lentil seeds. *Journal of Agricultural Engineering Research* [online]. 1996, **63**, 87–92. Dostupné z: https://ac.els-cdn.com/S0021863496900104/1-s2.0-S0021863496900104-main.pdf?_tid=499c8726-6117-449c-8704-28eb2730c846&acdnat=1545251269_235ee7464316674e764e94a009f0c5f7

[90] EMAMI, S. a L. G. TABIL. Friction and compression characteristics of chickpea flour and components. *Powder Technology* [online]. 2008, **182**, 119–126. ISSN 00325910. Dostupné z: doi:10.1016/j.powtec.2007.07.012

[91] YAN, H. a G. V. BARBOSA-CÁNOVAS. Compression characteristics of agglomerated food powders : Effect of agglomerate size and water activity Caracter & iacute ; sticas de la compresi & oacute ; n de. *Food Science and Technology International*. 1997, **3**, 351–359.

[92] RAJI, A.O. a J.F. FAVIER. Model for the deformation in agricultural and food particulate materials under bulk compressive loading using discrete element method . I : Theory , model development and validation. *Journal of Food Engineering* [online]. 2004, **64**, 359–371. Dostupné z: doi:10.1016/j.jfoodeng.2003.11.004

[93] OZBAY, A. a A. F. CABALAR. Effects of triaxial confining pressure and strain rate on stick-slip behavior of a dry granular material. *Granular Matter* [online]. 2016, **18**(3), 1–9. ISSN 14347636. Dostupné z: doi:10.1007/s10035-016-0664-7

[94] SARUMI, M. A. a S. T S AL-HASSANI. High and low strain rate properties of powders for continuum analysis. *Powder Technology* [online]. 1991, **65**, 51–59. ISSN 00325910. Dostupné z: doi:10.1016/0032-5910(91)80168-I

[95] MITTAL, Bhavishya a V. M. PURI. Rate-dependent elasto-viscoplastic constitutive model for industrial powders. Part 1: Parameter quantification. *Particulate Science and Technology* [online]. 2005, **23**(3), 249–264. ISSN 02726351. Dostupné z: doi:10.1080/02726350590955895

[96] KULIG, Ryszard, Grzegorz ŁYSIAK a Stanisław SKONECKI. Prediction of pelleting outcomes based on moisture versus strain hysteresis during the loading of individual pea seeds. *Biosystems Engineering* [online]. 2015, **129**(2004), 226–236. ISSN 15375110. Dostupné z: doi:10.1016/j.biosystemseng.2014.10.013

[97] STASIAK, M., K. SKIBA, M. MOLENDA, J. TYS a L. MOŚCICKI. The mechanical parameters of rapeseed cake. *Energy Sources, Part A: Recovery, Utilization and Environmental Effects* [online]. 2012, **34**(13), 1196–1205. ISSN 15567036. Dostupné z: doi:10.1080/15567031003773247

8. Appendices

Appendix A

List of Publications

Fresh Manuscripts For Publication in Peer-Reviewed Journals

1. Akangbe, O.L., Blahovec, J., Adamovský, R., Linda, M. and Hromasova, H. (**Under Review**). Effects of selected process parameters on the compaction of carob powder. ***Agronomy Research***.
2. Akangbe, O.L., Blahovec, J., Adamovsky, R. Phenomenological approach to the densification of food powders. **PT**
3. Akangbe, O.L., Blahovec, J., Adamovsky, R., Linda, M. Wall friction during high pressure densification of selected functional food materials. **SAB/JFPE**
4. Akangbe, O.L., Adamovský, R., Blahovec, J., Rutkowski, K. (**Accepted**). Densification behaviour of carob powder. ***INFRAECO***, NOT INDEXED ON SCOPUS

Fresh Manuscript For Publication as Article in Peer-Reviewed Conference Proceedings

5. Akangbe, O.L., Blahovec, J., Adamovský, R., Linda, M. and Hromasova, H. A device to measure wall friction during uniaxial compression of biomaterials. ***7th International Conference on Trends in Agricultural Engineering***.

Achieved Publications in Peer-Reviewed Journals

1. Akangbe, O. L., Adamovsky, R., & Mosna, F. (2018). Optimising cold compressive recovery of oil from the seeds of Sesame (Sesamum indicum L .). ***Agronomy Research***, 16(3), 634–645.

2. Akangbe, O. L., & Herak, D. (2017). Mechanical behaviour of bulk seeds of some leguminous crops under compression loading. ***Scientia Agriculturae Bohemica***, 48(4), 238–244. https://doi.org/10.1515/sab-2017-0031

3. Akangbe, O. L., & Herák, D. (2017a). Mechanical behaviour of selected bulk oilseeds under compression loading. ***Agronomy Research***, 15, 988–993. https://doi.org/10.22616/ERDev2017.16.N206

4. Akangbe, O. L., & Herák, D. (2018). Compressive stress, repetitive strain, and optimum expression of oil from bulk volumes of sesame seeds. ***Journal of Food Process Engineering***, 41(4), e12682. https://doi.org/10.1111/jfpe.12682

5. Kabutey, A., Herak, D., Choteborsky, R., Dajbych, O., Sigalingging, R., & Akangbe, O. L. (2017). Compression behaviour of bulk rapeseed: Effects of heat treatment, force, and speed. ***International Journal of Food Properties***, 20, S654–S662. https://doi.org/10.1080/10942912.2017.1306555

6. Kabutey, A., Herak, D., Choteborsky, R., Mizera, C., Sigalingging, R., & Akangbe, O. L. (2017). Oil point and mechanical behaviour of oil palm kernels in linear compression. ***International Agrophysics***, 31(3), 351–356. https://doi.org/10.1515/intag-2016-0055

Achieved Publications in Peer-Reviewed Conference Proceedings

7. Akangbe, O. L., & Adamovsky, R. (2018). Some process parameters affecting the densification of oleaginous biomaterials. In Book of Abstracts of the **17th International Workshop for Young Scientists "BioPhys Spring** 2018" (p. 9). Nitra, Slovakia.

8. Akangbe, O. L., & Herák, D. (2017b). Oil point determination of selected bulk oilseeds under compression loading. In V. Osadcuks (Ed.), Proceedings of the 16th **International Scientific Conference on Engineering for Rural Development** (pp. 988–993). Jelgava, Latvia.

9. Kabutey, A., Herák, D., Dajbych, O., Akangbe, O. L., Napitupulu, R., & Pandiangan, S. (2016). Mechanical behaviour of roasted and unroasted oil palm kernels under compression loading. In Proceedings of the **International Symposium on Agricultural and Mechanical Engineering** (Vol. 6, pp. 11–14). Bucharest.

10. Kabutey, A., Herák, D., Hanus, J., Choteborsky, R., Dajbych, O., Sigalingging, R., & Akangbe, O. L. (2016). Prediction of pressure and energy requirement of Jatropha Curcas L bulk seeds under non-linear pressing. In **6th International Conference on Trends in Agricultural Engineering** (pp. 262–269). Prague.

Appendix B

Calibration chart for the friction acquisition device

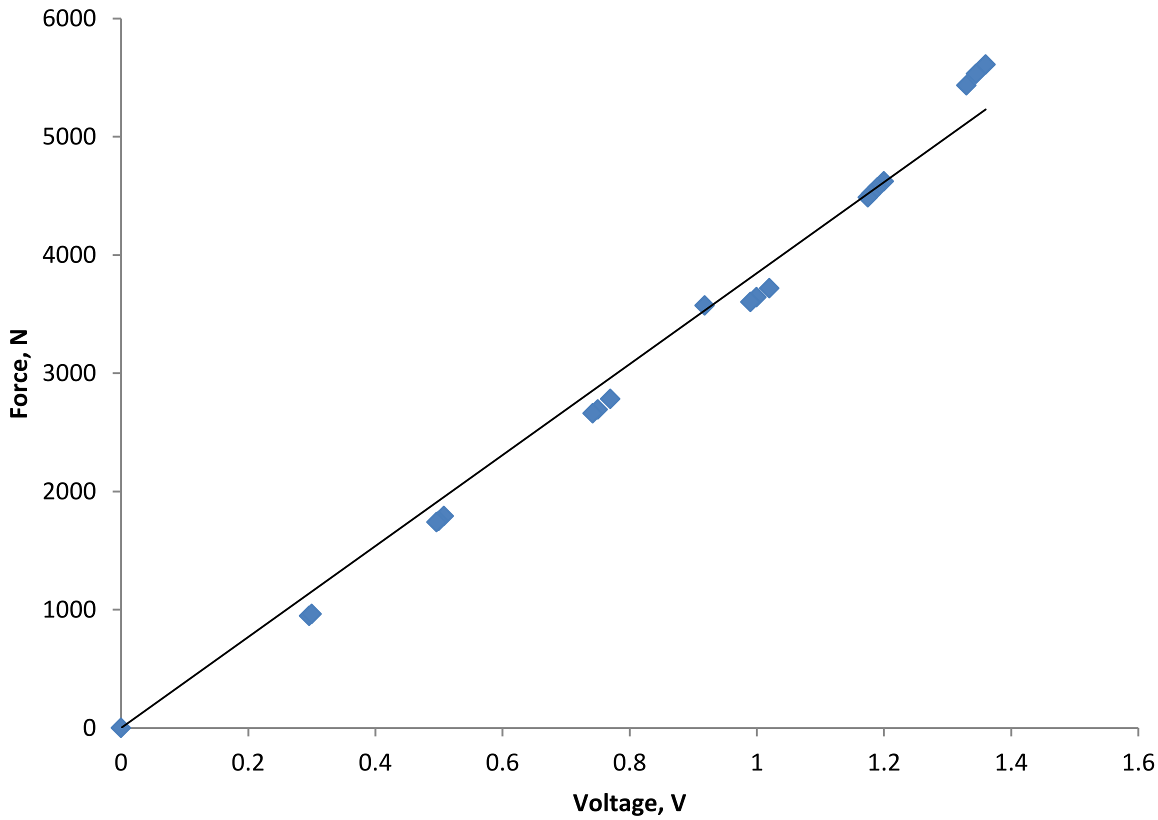

Appendix C

Stripped components of the friction force sensing device and compression die support